NUREG/CR-2673
ORNL/TM-8306

ornl

OAK RIDGE NATIONAL LABORATORY

UNION CARBIDE

Evaluation of Thermal Devices for Detecting In-Vessel Coolant Levels in PWRs

J. E. Hardy
C. E. Davis
K. G. Turnage
R. L. Anderson

Prepared for the U.S. Nuclear Regulatory Commission
Office of Nuclear Regulatory Research
Under Interagency Agreements DOE 40-551-75 and 40-552-75

OPERATED BY
UNION CARBIDE CORPORATION
FOR THE UNITED STATES
DEPARTMENT OF ENERGY

Printed in the United States of America. Available from
National Technical Information Service
U.S. Department of Commerce
5285 Port Royal Road, Springfield, Virginia 22161

Available from

GPO Sales Program
Division of Technical Information and Document Control
U.S. Nuclear Regulatory Commission
Washington, D.C. 20555

NUREG/CR-2673
ORNL/TM-8306
Dist. Category R2

Contract No. W-7405-eng-26

Engineering Technology Division

EVALUATION OF THERMAL DEVICES FOR DETECTING IN-VESSEL COOLANT LEVELS IN PWRs

J. E. Hardy
C. E. Davis
K. G. Turnage
R. L. Anderson

Manuscript Completed - July 29, 1982
Date Published - August 1982

Prepared for the
U.S. Nuclear Regulatory Commission
Office of Nuclear Regulatory Research
Under Interagency Agreements DOE 40-551-75 and 40-552-75

NRC Fin No. B0401

Prepared by the
OAK RIDGE NATIONAL LABORATORY
Oak Ridge, Tennessee 37830
operated by
UNION CARBIDE CORPORATION
for the
DEPARTMENT OF ENERGY

CONTENTS

ACKNOWLEDGMENTS

This research and development was performed at Oak Ridge National Laboratory, operated by Union Carbide for the Department of Energy. This work was part of the Advanced Two-Phase Flow Instrumentation Program under the sponsorship of the U.S. Nuclear Regulatory Commission (NRC). In particular this work was directed by the Division of Accident Evaluation, Experimental Programs Branch. The authors wish to acknowledge the assistance and direction of NRC staff members A. L. M. Hon and Y. Y. Hsu.

Numerous members of the laboratory staff were essential in completion of this task. The authors express a deep appreciation to the following persons for their efforts:

W. H. Glover, III
P. H. Hayes
H. W. Hoffman
J. D. Lyons
R. W. McCulloch
F. R. Mynatt
D. G. Thomas
H. E. Trammell

EVALUATION OF THERMAL DEVICES FOR DETECTING IN-VESSEL COOLANT LEVELS IN PWRs

J. E. Hardy K. G. Turnage
C. E. Davis R. L. Anderson

ABSTRACT

From investigations conducted immediately after the Three Mile Island nuclear power plant accident, some safety areas needing improvement were identified. One new Nuclear Regulatory Commission requirement was the unambiguous detection of the approach to adequate core cooling. Designs to meet this requirement have generally included new instrumentation to monitor the coolant level in the reactor vessel. Thermal sensors proposed for use in pressurized-water reactor (PWR) vessels were tested and evaluated. The thermal devices tested use pairs of K-type thermocouples or resistance temperature detectors to sense the cooling capacity of the medium surrounding the device. One sensor of the pair is heated by an electric current, while the unheated one senses the ambient fluid temperature. The temperature difference between the heated and unheated sensors provides an indication of the cooling capacity of the surrounding fluid. Experiments that simulated the thermal-hydraulic conditions of a postulated PWR loss-of-coolant accident (LOCA) were run, including both natural- and forced-convection two-phase flow tests. Results suggest that thermal level devices generally indicate the existence of poor cooling conditions in LOCA environments. In some cases, however, the indication of the thermal devices may not be a direct measurement of water level. Shielding and separator tubes have been devised to ensure that the thermal sensors indicate the collapsed liquid level inside the separator tube. Preliminary evaluation of these protection systems is given.

---

1. INTRODUCTION

During the accident at the Three Mile Island (TMI) nuclear power plant, a condition of low water level in the reactor vessel and inadequate core cooling (ICC) was not recognized for a long time. A review of the accident was conducted by the U.S. Nuclear Regulatory Commission (NRC) TMI-2 Lessons Learned Task Force.[1] Their report recommended that improved instrumentation systems, possibly including reactor-vessel liquid level (coolant) sensors, be developed and implemented in all pressurized-water reactors (PWRs) in the United States.

As a part of the NRC Action Plan[2] following the TMI accident, the Advanced Two-Phase Flow Instrumentation (ATPI) Program at Oak Ridge National Laboratory (ORNL) was funded by the NRC Division of Accident Evaluation to evaluate instrumentation systems for in-vessel level detection. The coolant level sensors are to detect the approach to or the extent of ICC. The requirements for these devices are

1. unambiguous indications (little operator interpretation required),
2. useful response under stagnant boiloff,
3. reliable [long life and survival of a loss-of-coolant accident (LOCA)], and
4. time response on the order of 1-2 min.

Additionally, the ICC instrumentation is to monitor the entire vessel.

Many instrumentation schemes were suggested for measuring liquid level. Some of the more notable ones are ultrasonic methods, differential pressure (ΔP), capacitance probes, time-domain reflectometry, and thermal devices, such as heated thermocouples (HTCs) and heated resistance temperature detectors (HRTDs). This report will deal only with HTCs and HRTDs.

The operation of heated thermal sensors is based on the large difference in heat transfer characteristics between liquid and vapor phases. This difference varies with both pressure and temperature. The HTCs use pairs of K-type thermocouples (TCs), while HRTDs use a pair of RTDs as sensors. One sensor of the pair is heated by a separate electric heater; the other, unheated junction is sufficiently removed from the heater so that it essentially detects the ambient fluid temperature. The temperature difference (ΔT) between the two sensors gives an indication of the cooling capacities of the medium surrounding the device. For a given heater power, under good cooling conditions (liquid or rapidly flowing two-phase mixtures), the ΔT will be relatively low. In poor cooling conditions (stagnant steam or other gas), the ΔT will be higher.

Thermal sensors have several attractive features. They measure cooling conditions directly; thus, inferences need not be made. They also use reactor-compatible materials, are relatively small, and are fairly simple and inexpensive. However, several disadvantages of thermal level detectors exist. The sensors give only discrete indications of level, and arrays are required to cover the entire vessel. Also, unshielded sensors can be cooled by entrained liquid above the liquid-vapor interface, and they may not be useful during normal operating conditions if connected as differential output only. Finally, there is the possibility that the heater may fail and render the detector useless.

To evaluate the advantages and disadvantages of the thermal sensor, many devices were tested including sensors designed and fabricated at ORNL as well as sensors procured from outside sources. Experiments were conducted that simulated thermal-hydraulic conditions typical of an LOCA, both natural-convection (reactor coolant pumps off) and forced-convection (pumps on) two-phase flow tests were run. Results of these tests showed that thermal sensors are viable instruments for in-vessel level detection. A few problems, however, were found and investigated. Conclusions and recommendations are given.

2. THERMAL DEVICES

2.1 Measurement Concepts

Two types of thermal devices, employing either the HTC or the HRTD concept, were evaluated at ORNL. Heated TCs were procured from outside sources as well as fabricated by ORNL personnel. The HRTDs were purchased from a commerical vendor, Fluid Components, Inc., Canoga Park, California.

The principle of operation for either thermal device is based on the fact that the thermal conductance of a liquid is greater than that of a gas or vapor. Figure 2.1 illustrates the difference in thermal conductivity between saturated steam and water as a function of temperature.[2] In the normal operating range of a PWR, the thermal conductivity of the

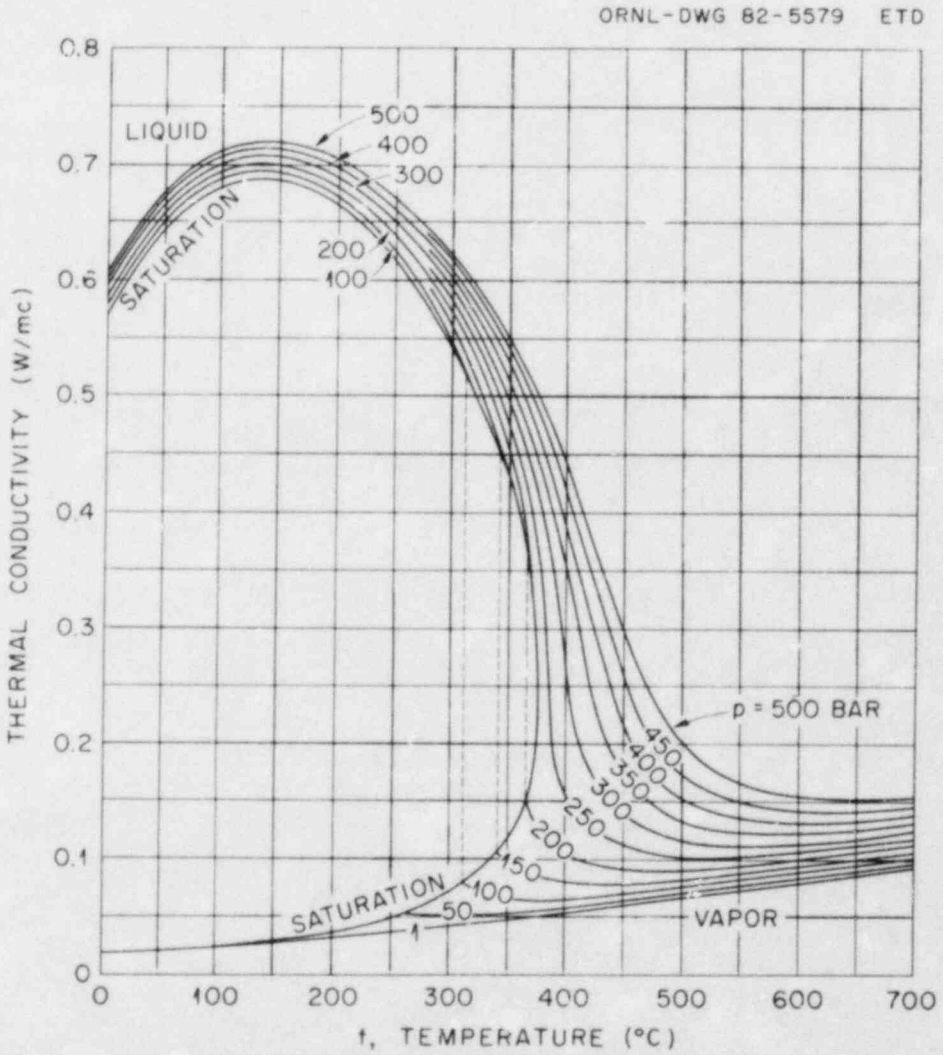

Fig. 2.1. Thermal conductivity k of water as liquid or vapor and as function of pressure and temperature.

liquid is a factor of 10 larger than that of saturated steam. Thus, the cooling capability of a liquid is much greater than that of a gas or vapor. The ability to remove heat from an object is directly related to the surrounding medium's thermal conductivity, and the heat removal rate is also strongly dependent on the fluid conditions (e.g., voiding, density, and temperature). Typically, a liquid or rapidly flowing two-phase mixture can remove heat fairly quickly whereas slow-moving or stagnant steam or other gas are poor heat transfer agents. A thermal coolant level device uses this difference in heat transfer rates to detect the cooling capacity of the medium in which it is located. Two thermal sensors are positioned in one detector, TCs or RTDs. A heater is situated in good thermal contact with one of the sensors. This heater, consisting of a single wire, is powered by an electrical current and increases the temperature of the nearest sensor. The ΔT between the heated and unheated sensor is a function of the heat transferred to the surroundings. If the heat is removed relatively quickly the ΔT will be small. However, if the heat transfer to the surroundings is poor the ΔT may be substantial and much larger than for the previous case. Thus, by monitoring the magnitude of the ΔT, the cooling condition at the probe location can be determined. A small ΔT indicates a high cooling capacity, and a large ΔT indicates poor cooling.

An important factor that also influences the ΔT between the heated and unheated junctions is the input power to the heater. The ΔT is also influenced by the probe design but to a lesser extent. The more power supplied to the heater, the larger the ΔT between the sensors for good and poor cooling, and the easier it becomes to distinguish between the two. This larger difference is especially helpful when water and steam are present at high temperatures and pressures. Steam's cooling effectiveness increases with pressure and begins to approach water's cooling capacity. A larger change between the ΔTs enables a more reliable judgment to be made as to the cooling condition. A trade-off must be made in heater power, however, because a combination of high power and poor cooling may overheat the device and damage the heater. This trade-off point is determined from probe design and materials, range of fluid conditions, and system pressure and temperature. Possible solutions to protecting the heater from damage are to limit the heater current or to control the magnitude of the ΔT.

2.2 Design and Fabrication

Five heated TC probes were designed and fabricated at ORNL. The first three were single-point measuring stations; the final two were multiple-position units, three and four stations, respectively. The HTCs were procured from Combustion Engineering (C-E) and Robinson Halpern Company, a manufacturer of thermal liquid level sensors for the U.S. Naval Reactors Program. Also, commercially available HRTDs were purchased from Fluid Components, Inc. The design and fabrication of the ORNL devices will be discussed first and will be followed by a brief discussion of the sensors procured from outside sources.

The basic design requirements for HTCs were (1) low heat generation in the heater leads, (2) high electrical insulation resistance between components, (3) good radial heat transfer, and (4) relatively poor axial heat transfer. The design of a basic HTC sensor consisted of a low-power wire heater wound on a ceramic core with a type-K differential TC. One TC junction was placed near the heated region, and the other was placed ~5 cm away. The ceramic core insulated the TC from the heater, and the heater was insulated from the 3-mm-OD thin-walled stainless steel sheath by a second ceramic insulator. The heater may be grounded or ungrounded. The ungrounded configuration requires that both heater leads be insulated from the sheath and thermoelements, and the grounded configuration eliminates one of the heater lead wires.

Time constraints were such that existing or readily available materials had to be used to fabricate the devices. Nichrome wire is an excellent heating element material and was readily available. Alumina (Al_2O_3), magnesia (MgO), or boron nitride (BN) core ceramics were considered. The best choice was crushable MgO, but it was not readily available in the required dimensions. Crushable BN cores were less desirable as a central insulator because of their relatively high thermal conductivity, which could result in excessive heat conduction between TC junctions. Hand-fired Al_2O_3 cores that fit the dimensional requirements were available. Their use, while acceptable, resulted in less than optimum heat flux uniformity. Stainless steel tubing for the clad was on hand and, after centerless grinding, fit the clad dimensional requirements.

Because of the need for good radial heat transfer in the heated region, BN preforms were used in the annular region surrounding the core; the unit was swaged to obtain high and uniform annular density and good contact between components in the heat flux path. The heating element was grounded to the clad, and an end plug was welded to seal the device.

Sensor ORNL I (Fig. 2.2) was fabricated using 0.25-mm (0.010-in.) Nichrome wire on an Al_2O_3 ceramic form. The heating coil was wound on a mandrel and slipped over the Al_2O_3. The heating element wire was extended on the surface of the Al_2O_3 to the terminal end. The type-K differential TC was fabricated by butt welding a 0.25-mm (0.010-in.) K+ wire to a K- wire, stringing this wire and a second K- wire through holes in the ceramic, and welding the two elements at the end of the ceramic to form the second junction. The assembly, ~46 cm (18 in.) in length, was then inserted in the clad, followed by the annular preforms. The preforms were crushed only in the region of the heating coil. Finally, the 0.5-cm region at the end of the heating coil (Fig. 2.2) was filled with BN powder, the heater wire was grounded to the end plug, and the end plug was welded.

The unit was then electrically inspected (heating element resistance, insulation resistance between TC, heater, and clad) and swaged a maximum of 0.2 mm (0.008 in.). A more severe swage would have crushed the hand-fired Al_2O_3 insulator and possibly destroyed the TC and heaters. The unit was then again electrically inspected, radiographed, infrared scanned, and dye checked in the welded region.

The second HTC coolant sensor, ORNL II, was built by the Fuel Rod Simulator Fabrication Group at ORNL. The design and components for this probe were similar to those used in the first differential HTC except for a few design improvements. The HTC junction was located directly under the heater windings (Fig. 2.3), instead of just outside the windings

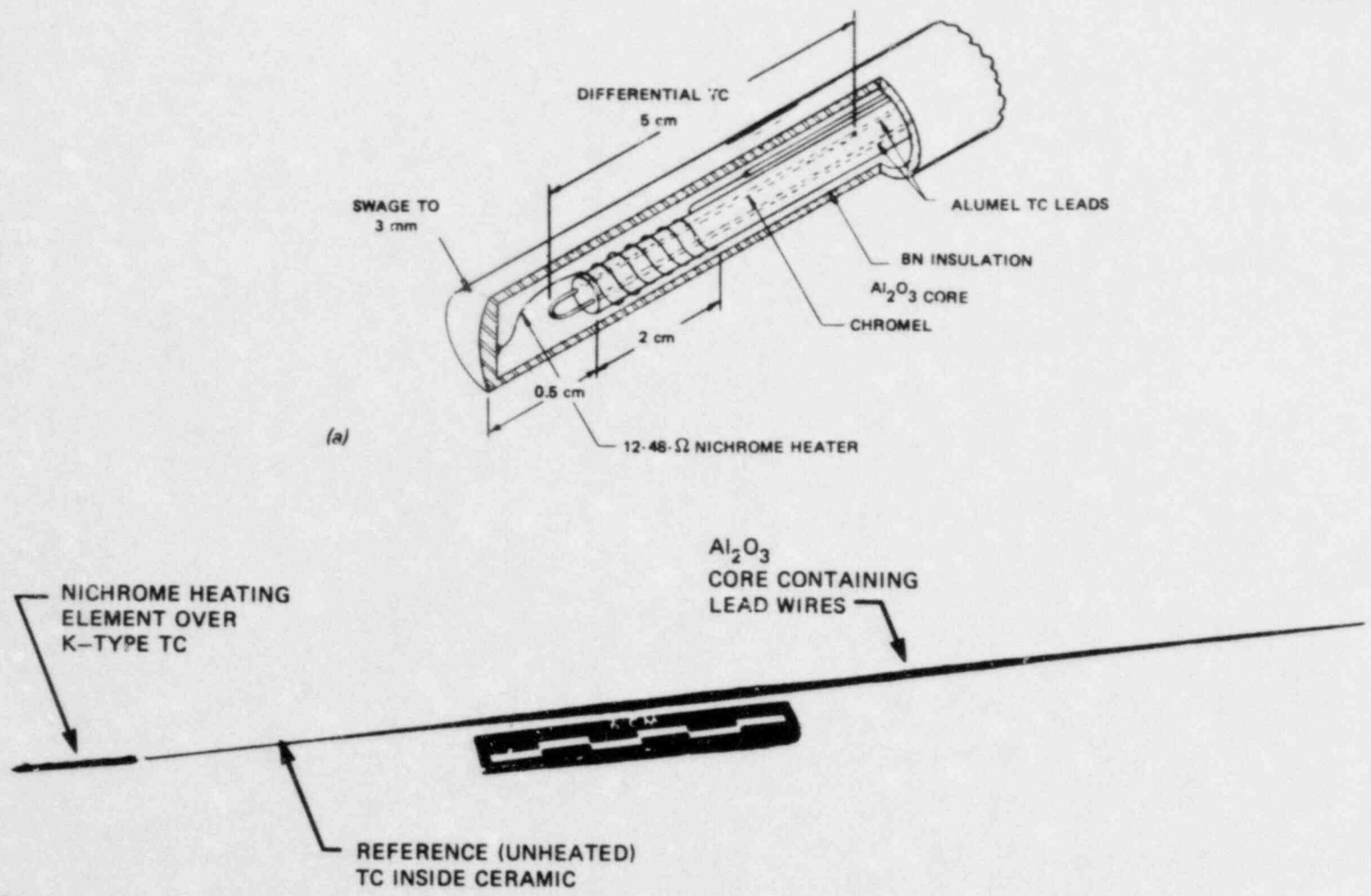

Fig. 2.2. (a) Drawing of prototype differential thermocouple liquid level probe and (b) photograph of internal heater and thermocouple assembly.

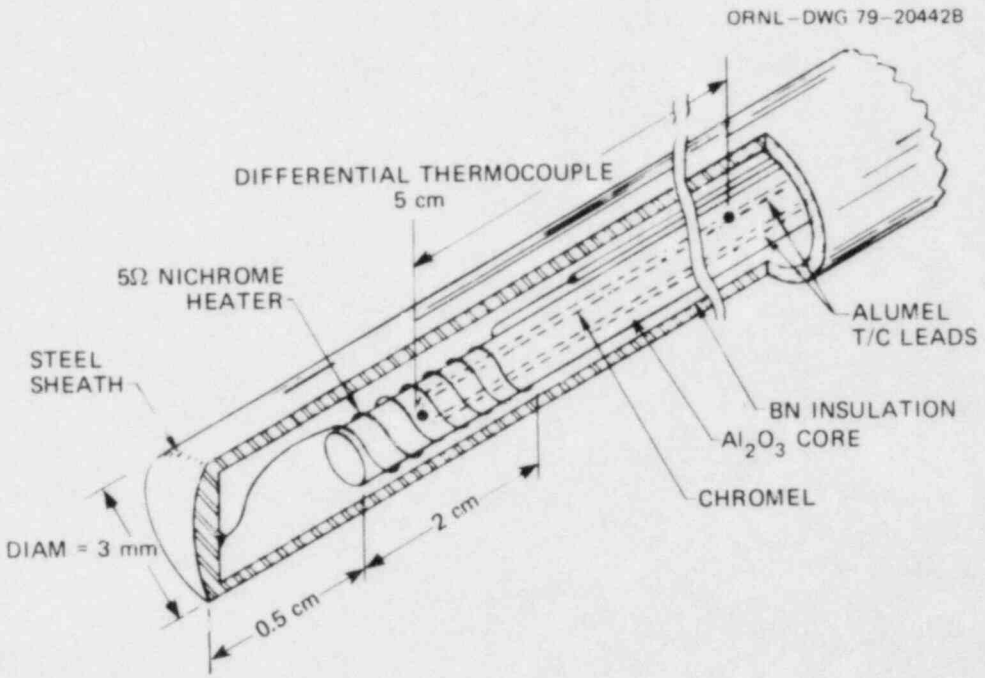

Fig. 2.3. HTC coolant sensor (ORNL II) fabricated by FRS Fabrication Group.

along the probe axis as in the first prototype. Compared with the earlier version, more heating of the hot junction will result, making the probe more sensitive to degradation of the surface heat transfer condition. A 0.13-mm-diam (0.005-in.) heater wire was used, and a 0.25-mm (0.010-in.) nickel lead wire was welded to it. This change was made to reduce the terminal heat generation.

The design of sensor ORNL III was modified substantially from the first two HTC probes. A four-thermoelement type-K section, ~63 cm (25 in.) in length and 3.175 mm (0.125 in.) in diameter, was used as the terminal end. This section was swaged to 2.79 mm (0.110 in.) to fit inside a 6.35-mm-OD (0.25-in.), 1.63-mm-wall (0.064-in.) tube. Crushable MgO insulators were used for the heater core material, and the heating wire was grounded by shim stock. Because of dimensional constraints, BN powder was used instead of preforms.

In practice, use of localized thermal-type sensors to follow liquid level will probably require insertion of a vertical array of sensors. A level probe was built containing an array of three HTCs.

The HTC array probe (Fig. 2.4) was 90 cm long, 6.4 mm in OD, with three heating elements centered at 5.7, 21.0, and 36.2 cm from one end. Heaters were made from 0.25-mm-diam Nichrome wire wound on 2.6-mm-diam alumina cores. A 0.5-mm-diam, type-K TC was located adjacent to each heater; three identical TCs were located halfway between heaters. Sauerisen adhesive cement paste was used as a filler between internal parts, but the unit was not swaged after assembly.

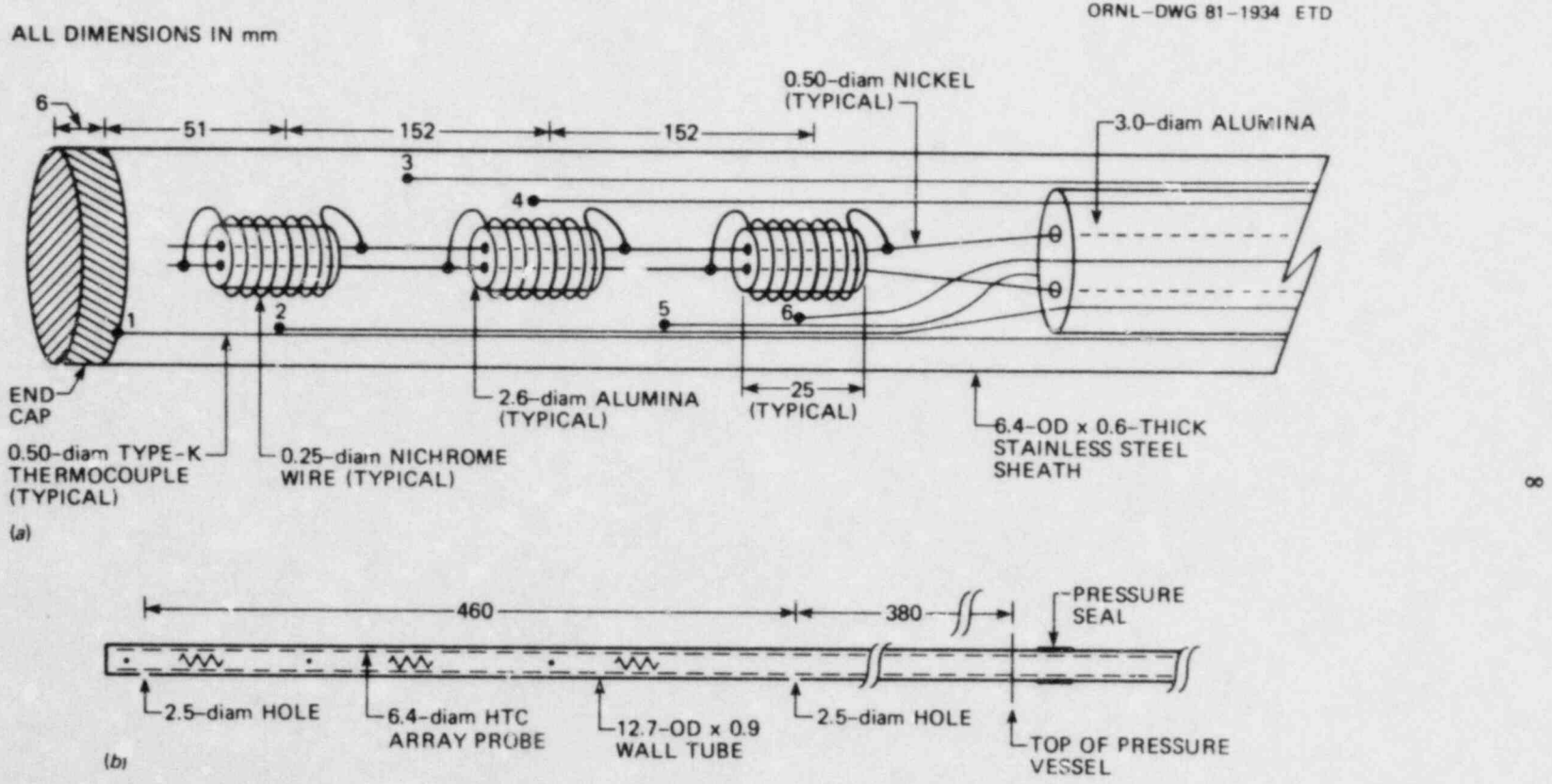

Fig. 2.4. Three-element HTC probe tested in pressurizer: (a) schematic view of probe internals and (b) overall view of probe.

A second multiple-position heated junction TC (MPHJTC) probe was designed and fabricated at ORNL (Fig. 2.5). The device contained four 2.5-cm sensors spaced at 20-cm axial intervals. Each sensor consisted of a heater wound with 0.25-mm-diam Nichrome V wire and two 0.38-mm-diam, type-K magnesia (MgO) insulated, 304 stainless steel sheathed TCs with high-density BN in their junction region. Their response time is ~20 ms. One thermocouple junction was located in the axial center of the 2.5-cm heater, and the other TC junction was located 10.0 cm away in the unheated region.

The TCs were attached to the HTC clad, which was insulated in the annular region from the four heated sections by high-density BN preforms. The TCs were connected so that both ΔT and absolute readings could be obtained. This arrangement provided a very sensitive indication of the fluid condition and, in conjunction with the heater, would provide a very sensitive level indication.

The four heaters were wound on 3.13-cm-OD crushable MgO insulators and connected in parallel by two 0.6-mm-diam copper bus bars, contained within holes in the center of the MgO insulators. Crushable 3.6-mm-diam MgO insulators were positioned between heater coils and in the terminal section.

The device was fabricated by (1) assembling the MgO crushable insulators, heater coils, and copper bus bars; (2) assembling the TCs within the clad with their junctions located at the precise axial location; (3) loading annular cold-pressed BN preforms; and (4) swaging the entire assembly. The end plug was then joined to the sensor after it had been given the required bend in the terminal region.

The MPHJTC was fabricated under strict quality controls including checks of heater and insulation resistance, critical process steps, and welds and braze connections.

The designs of the Navy-type and C-E HTCs were essentially the same as the ORNL HTCs. There were differences, however, in sizes and materials. Two thermal-type liquid level-interface monitors with resistive thermometers connected differentially were purchased from Fluid Components. One was of standard size, and the second HRTD design was miniaturized.

The standard sensor consists of a body, which contains the electrical connections for the heater and RTDs, and a sensor head (Fig. 2.6). The sensor head contains a pair of cylinders, connected on one end to the probe body and on the other end by a support bar. One pair of cylinders contains a heating element and an RTD that is in good thermal contact with the heater. Separated by a short distance from the heated assembly, the other pair of cylinders contains an RTD that is used as a temperature reference.

The miniaturized HRTD is functionally the same as the standard size device. The difference is that this probe is only 1.0 cm in OD, as compared with ~3 cm for a standard HRTD. The smaller HRTD consisted of a sensor head and body. The head contained two RTDs and a heater assembly. This miniaturized thermal sensor is shown in Fig. 2.7.

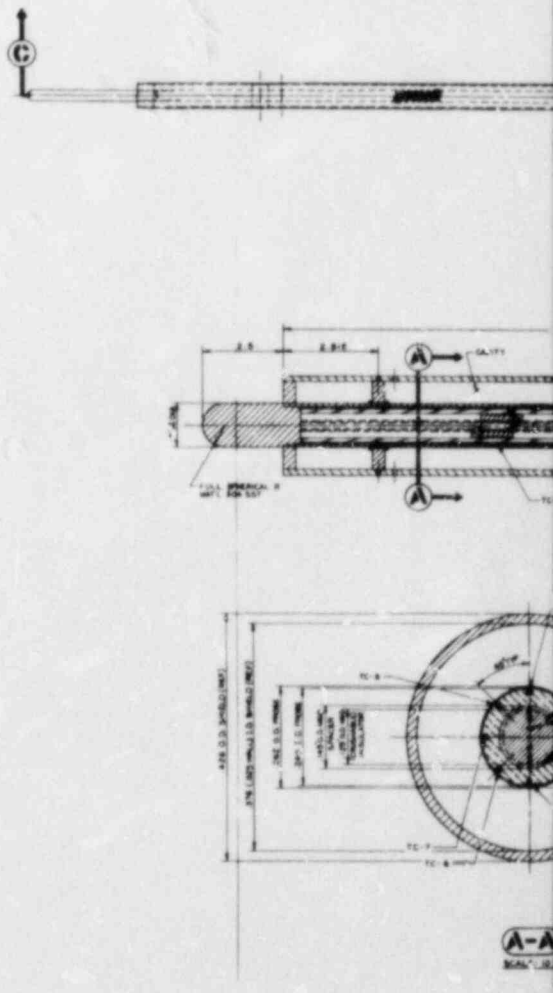

Fig. 2

ORNL–DWG 81–8269 ETD

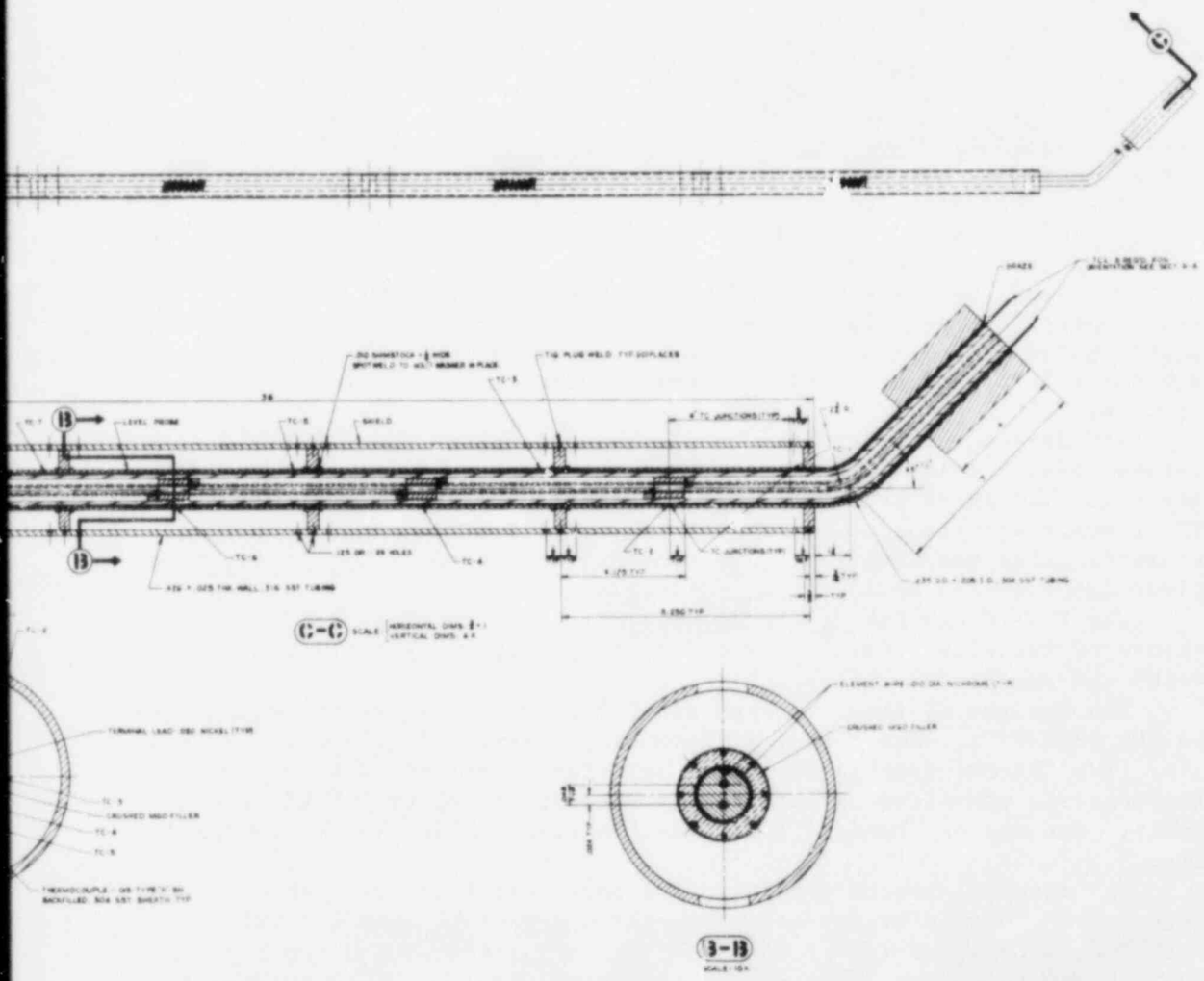

. Multiple-position heated junction thermocouple.

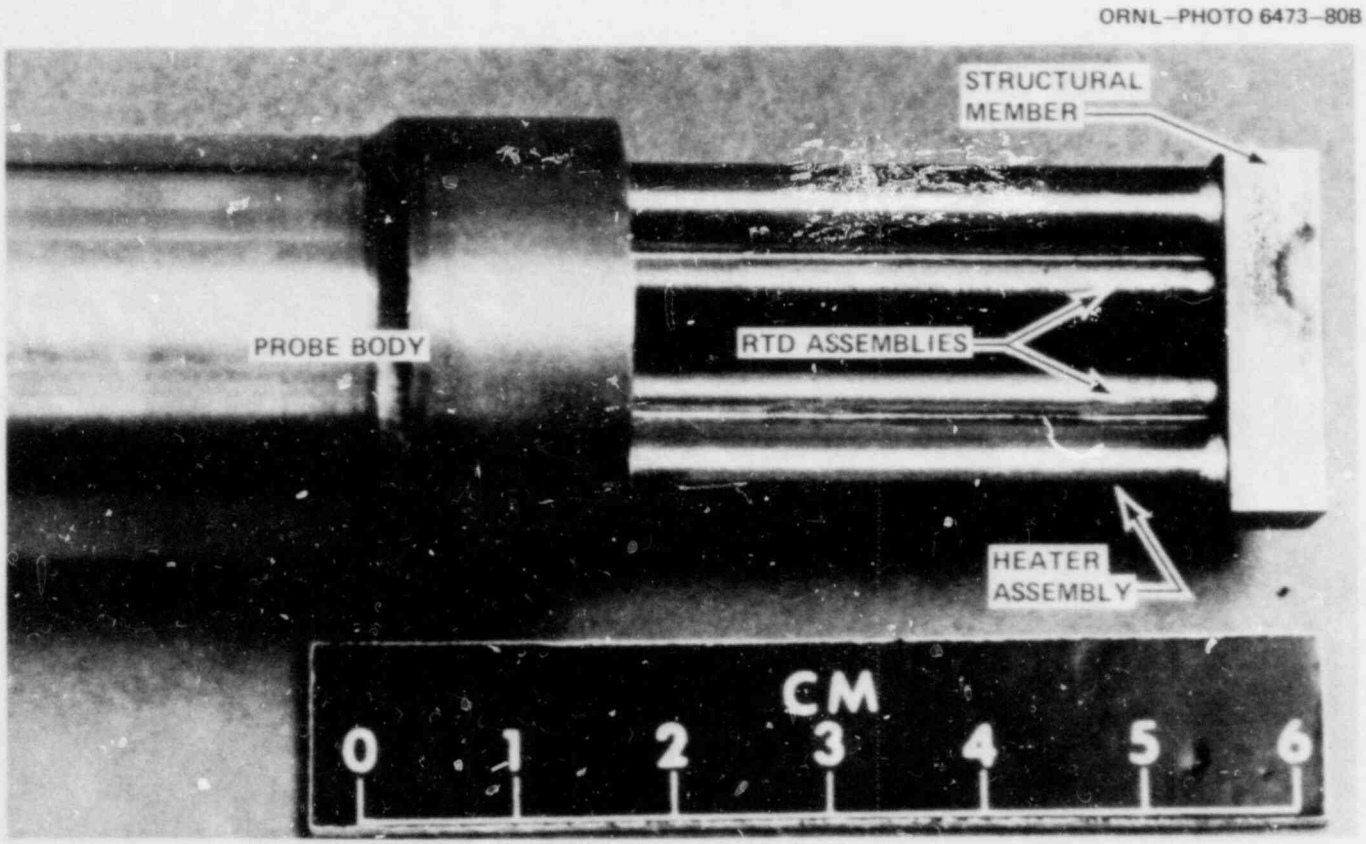

Fig. 2.6. Sensor head of commercial HRTD.

ORNL PHOTO 7043-80

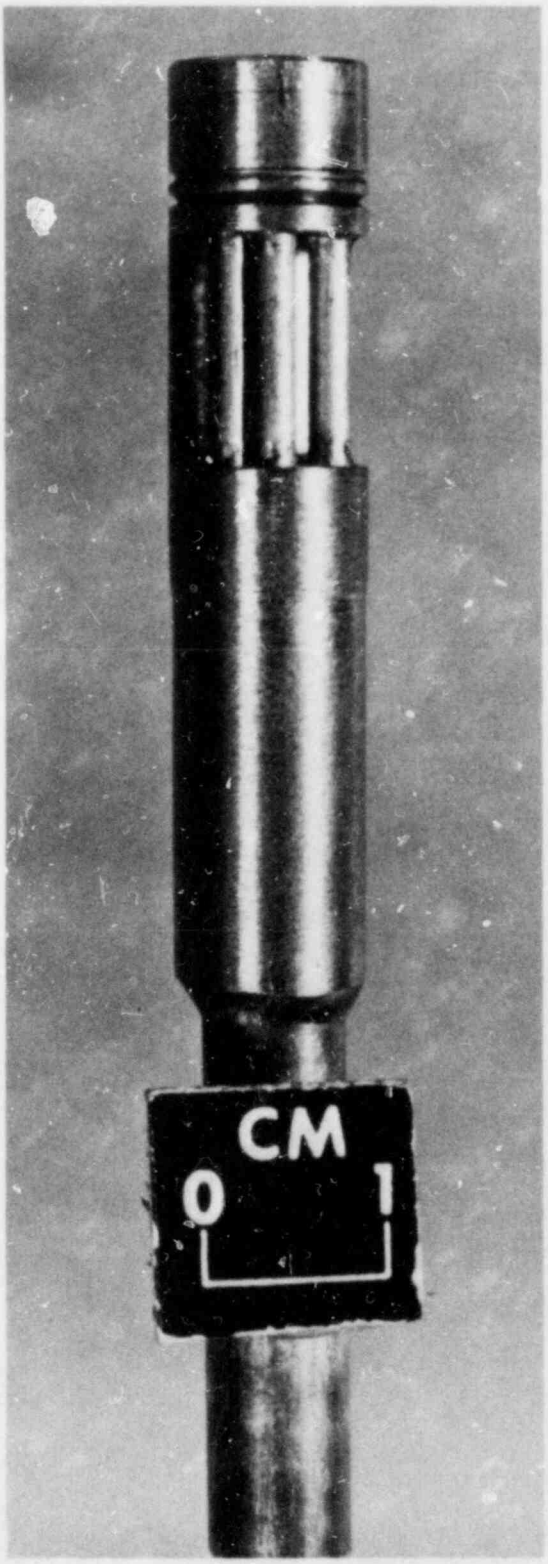

Fig. 2.7. Sensor head of miniaturized HRTD. Active region of probe is ~1 cm from top.

3. EXPERIMENTAL TEST FACILITIES

Several experimental facilities were employed in testing the thermal devices: the Air/Water Test Facility (AWTF); the Three-Module Air/Water Instrument Development Loop (3-Mod A/W IDL); the Steam/Water Pressurizer; the Steam/Water Flow Visualization Loop; the Advanced Instrumentation for Reflood Studies (AIRS) Steam/Water Test Stand; and the Thermal-Hydraulic Test Facility (THTF). These facilities provided a wide variety of testing modes and flow conditions. Many parameters could be varied in these experimental loops including pressure, temperature, flow (stagnant to high velocity), media (steam, air, or water), and geometry.

3.1 Air/Water Test Facility

A schematic diagram of the AWTF is shown in Fig. 3.1. The facility is constructed of polyvinyl chloride piping, most of which is clear to allow flow visualization. Water inputs are metered by either rotameter or an electromagnetic flowmeter. The flow rate ranges from 0.13 to 32 kg/s (2 to 500 gpm). Air flow is measured by a critical-flow orifice station containing four separate orifices that cover flow rates from 0.001 to 0.33 m^3/s (2 to 700 scfm). The loop operates at ambient temperature and pressure. A wide variety of flow rates, void fractions, and flow regimes can be produced.

3.2 Three-Module Air/Water IDL

The 3-Mod A/W IDL represents a vertical section from spray nozzles to the top of the upper plenum of a PWR. This facility is used to simulate flows at the core-upper plenum interface during the refill-reflood phase of an LOCA. A schematic of the loop is shown in Fig. 3.2 along with the location of the HTCs during testing. Air and water entered the bottom of the test vessel through three air-water mixers, which individually fed each module. Input air and water flow rates were monitored by vortex and/or turbine flowmeters. This facility was operated at ambient temperature, and maximum pressures in the vessel were <41 kPa (6 psig).

At approximately the same upper plenum elevation as the HTC test position, a low-energy gamma densitometer was installed with the source at the vessel centerline and the detector mounted on an outside wall of the vessel. This enabled void fraction measurements to be taken in the vicinity of the HTC.

3.3 Steam/Water Pressurizer

The Steam/Water Pressurizer was chosen as a test rig because a high-temperature, high-pressure environment (300°C, 10 MPa) could be obtained as well as a saturated steam/water interface that could be varied over the

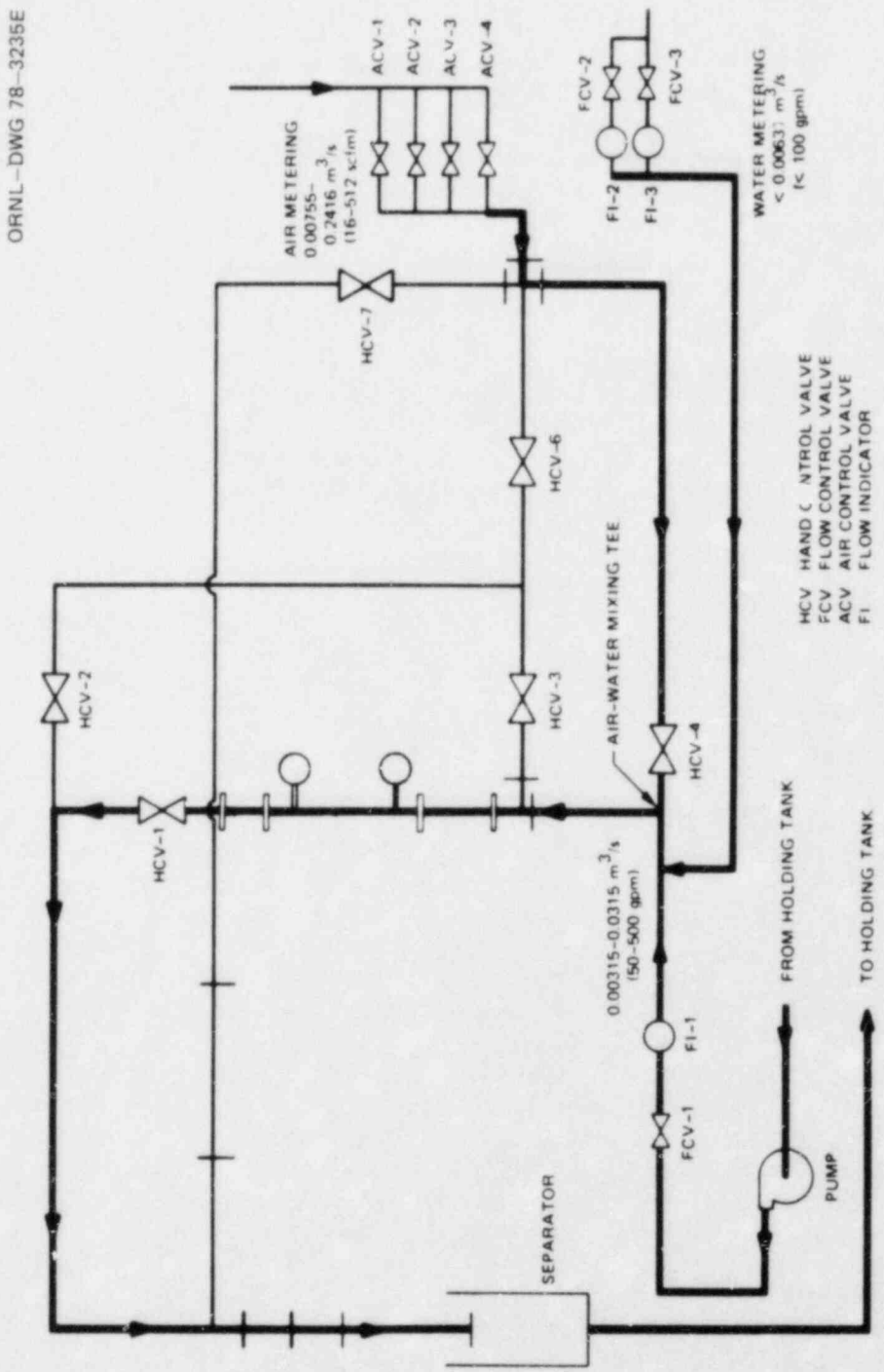

Fig. 3.1. Schematic of AWTF.

ORNL-DWG 79-60€2B ETD

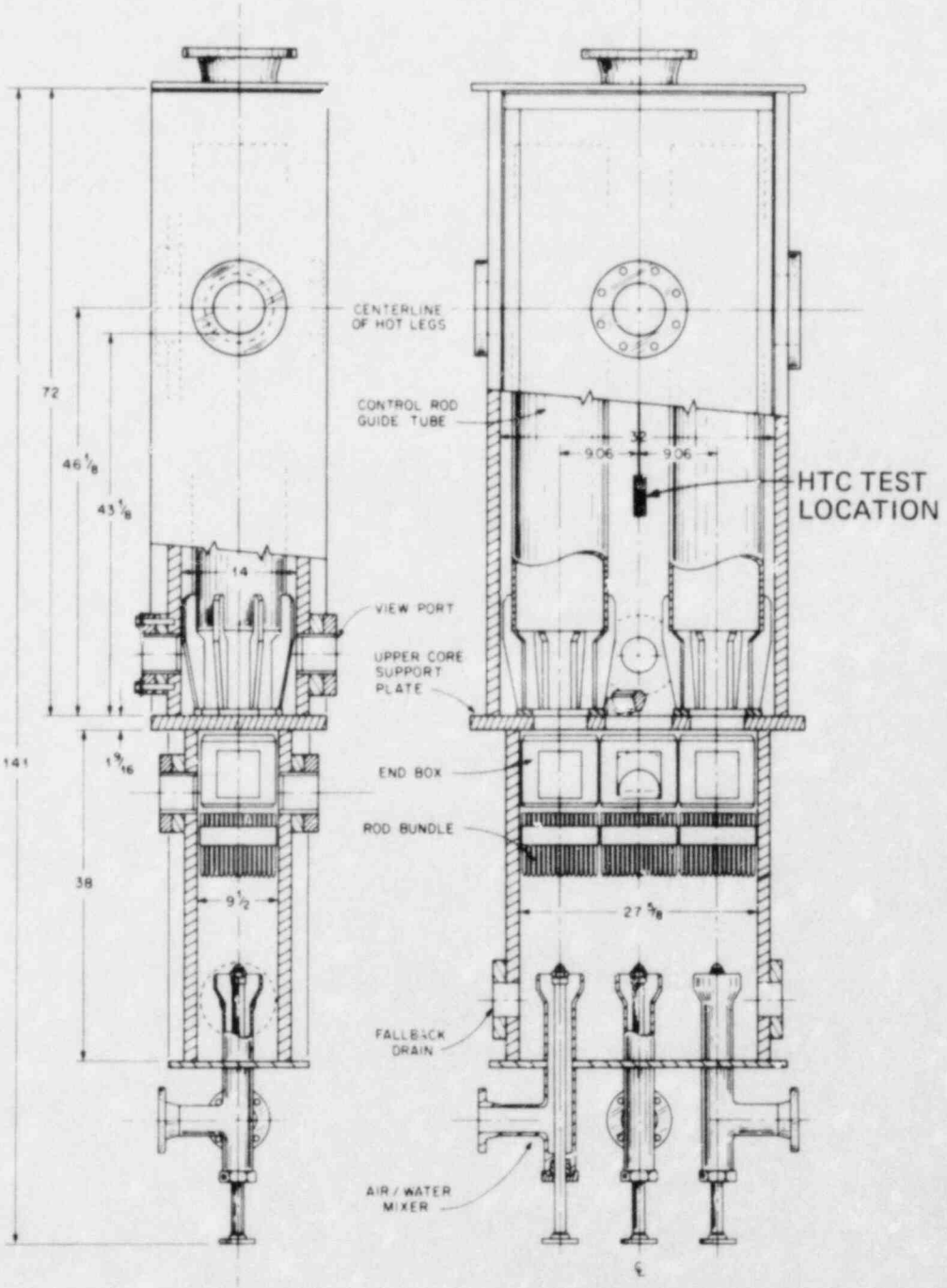

Fig. 3.2. Three-module Air/Water IDL.

height of the vessel. A schematic diagram with various thermal coolant level sensor ports is given in Fig. 3.3. The pressurizer is a 13-cm-ID cylindrical vessel with a height of ~1.1 m. The pressurizer was part of the Transient Instrumentation Test Facility (TITF), used to evaluate transient two-phase sensors. An independent, accurate indication of the water level in the pressurizer was obtained using a pressure difference-level (ΔP) system. The location of the taps are shown in Fig. 3.3. Figure 3.4 contains a photograph of the pressurizer. For level probe testing, the system was pressurized using strip heaters mounted on the pressurizer body; then the liquid level sensors were covered and uncovered with saturated water using system letdown valves and a high-pressure injection pump (Fig. 3.3).

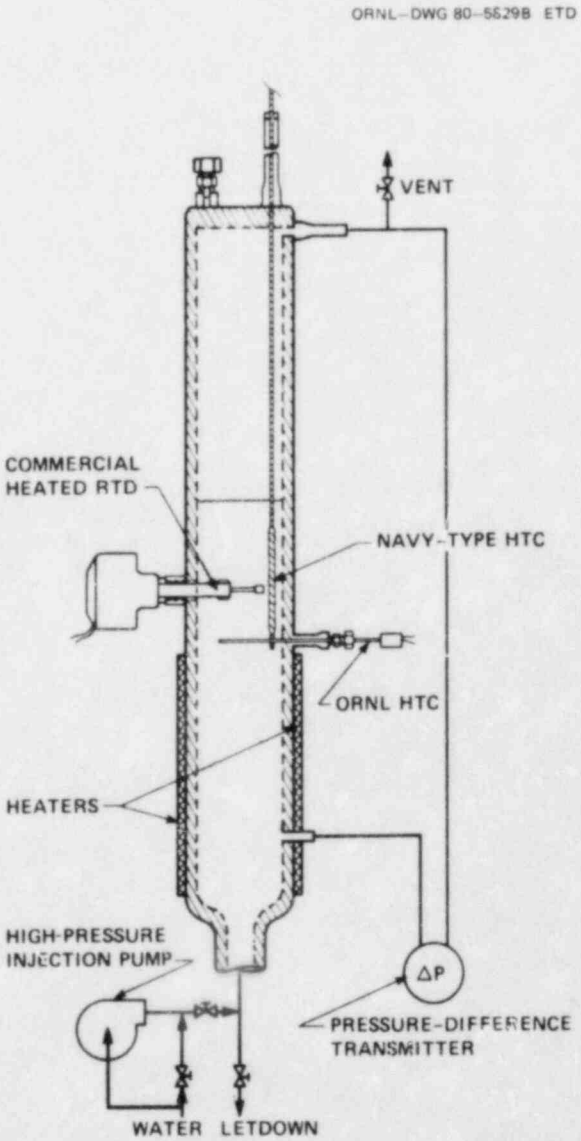

Fig. 3.3. Schematic of test section used for high-pressure natural-convection experiments with thermal liquid level sensors.

ORNL–PHOTO 6441–80B

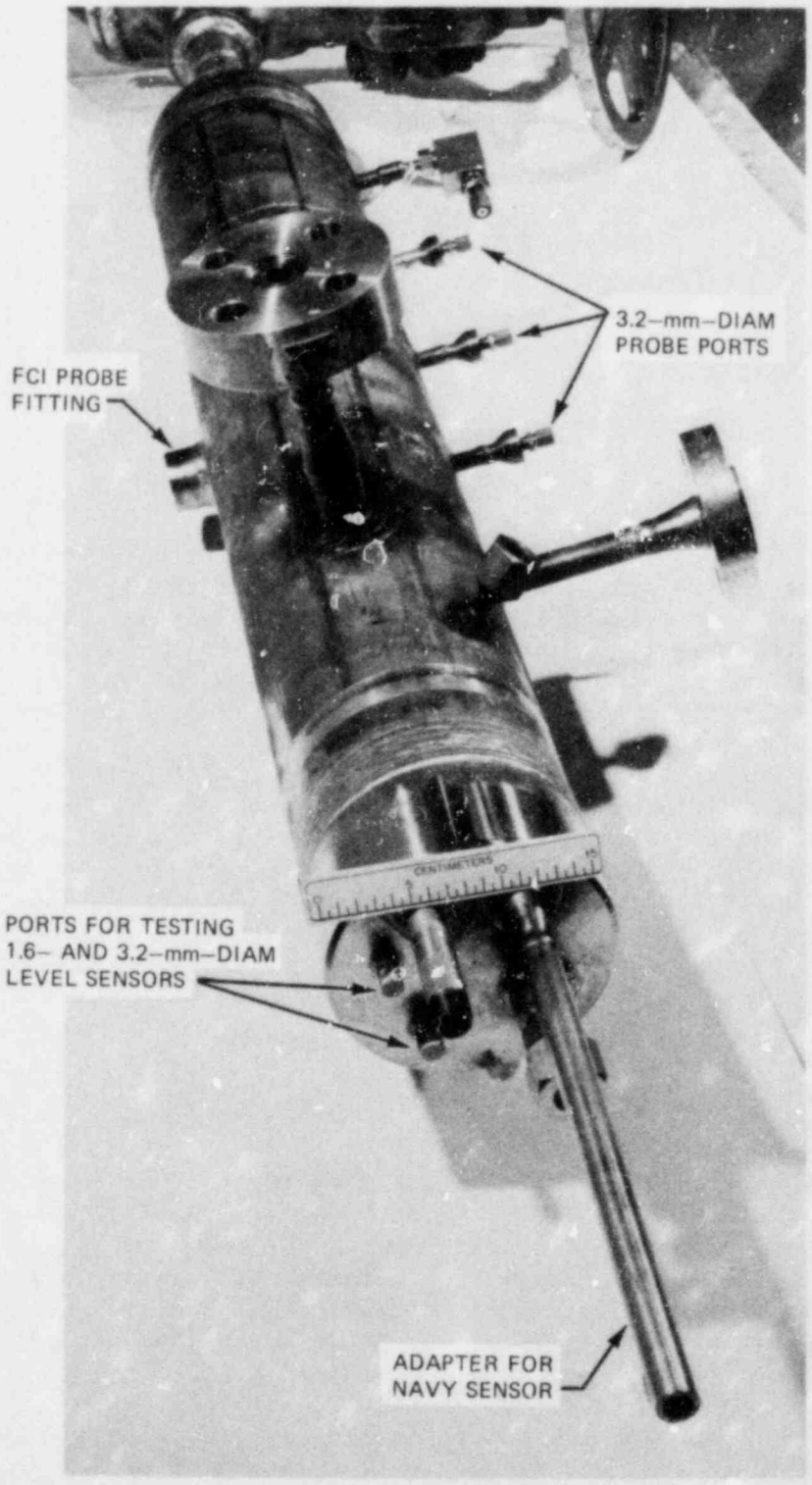

Fig. 3.4. Steam/water pressurizer used in evaluating thermal liquid level sensors.

3.4 Steam/Water Flow Visualization Loop

The test section of the flow visualization facility is constructed of 10-cm-ID polysulfone (TM) piping. A 20-mm-thick perforated plate (the tie plate) with 10.5-mm-diam holes on a 14.5-mm² pitch was installed (Fig. 3.5).

During testing, subcooled water enters the test section from above, while steam flows from below. Various flow rates of steam and water may be used to produce variable-density froths and droplet flow regimes in the region above the tie plate. Tests performed in the low-pressure countercurrent flow facility were useful in characterizing thermal probe output behavior, while simultaneously observing the steam-water flow regime through transparent test section walls.

3.5 AIRS Steam/Water Test Stand

The steam/water test stand was designed to duplicate refill-reflood flow conditions. The test stand operated at pressures up to 1 MPa (150 psig) and temperatures to 170°C (338°F). The input steam flow was measured by a Gilflo meter (variable-area orifice meter), and input water was metered by turbine flowmeters. Maximum steam flow was ~1.1 kg/s [a superficial steam velocity of ~30 m/s (100 ft/s)], and the maximum water rate was 1.3 kg/s (20 gpm).

The test stand (Fig. 3.6) was a once-through cocurrent steam-water flow system ~10 m in overall height. The HTCs were tested in a horizontal orientation at the location shown in Fig. 3.6. An instrumented spool piece 1 m long was directly upstream of the thermal sensors. The instrumented spool contained a pressure tap, TC, triple-beam gamma densitometer, and a full-flow turbine meter. The densitometer provided a chordal average void fraction 80 cm below the test probe. The full-flow turbine gave an indication of the pipe average velocity in two-phase flow.

3.6 Thermal-Hydraulic Test Facility

The THTF is a high-pressure single-loop separate-effects facility designed to simulate some aspects of an LOCA. In the THTF, an 8 x 8 square array of 3.7-m-long electrically heated rods geometrically models part of a 17 x 17 PWR fuel assembly. The THTF rod bundle is instrumented to allow accurate determination of local electric fuel rod simulator (FRS) surface temperatures and heat fluxes. An array of TCs is used to measure fluid temperatures at the rod bundle outlet (Fig. 3.7). Fluid density measurements in the outlet piping of the facility were made with two gamma densitometers. A turbine flowmeter provided an indication of the volumetric flow rate at the test section outlet.

A differential-type HTC was installed in the THTF upper plenum near the test section outlet nozzle (Fig. 3.7). The THTF was operated under transient or quasi-steady-state conditions over a range of pressures from

ORNL PHOTO 6439-80A

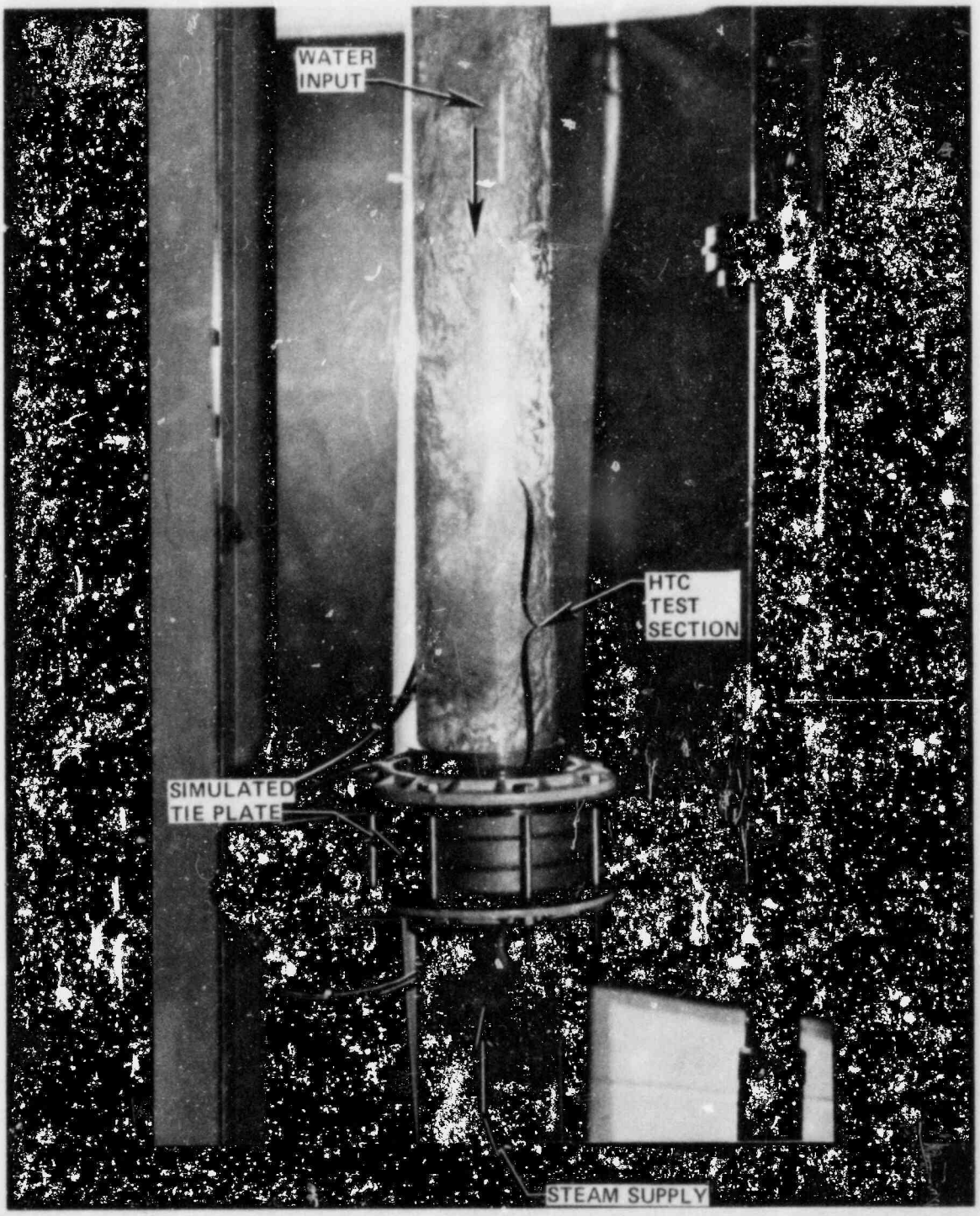

Fig. 3.5. Low-pressure countercurrent test facility used for observing steam/water two-phase flow regimes during testing of thermal coolant sensor.

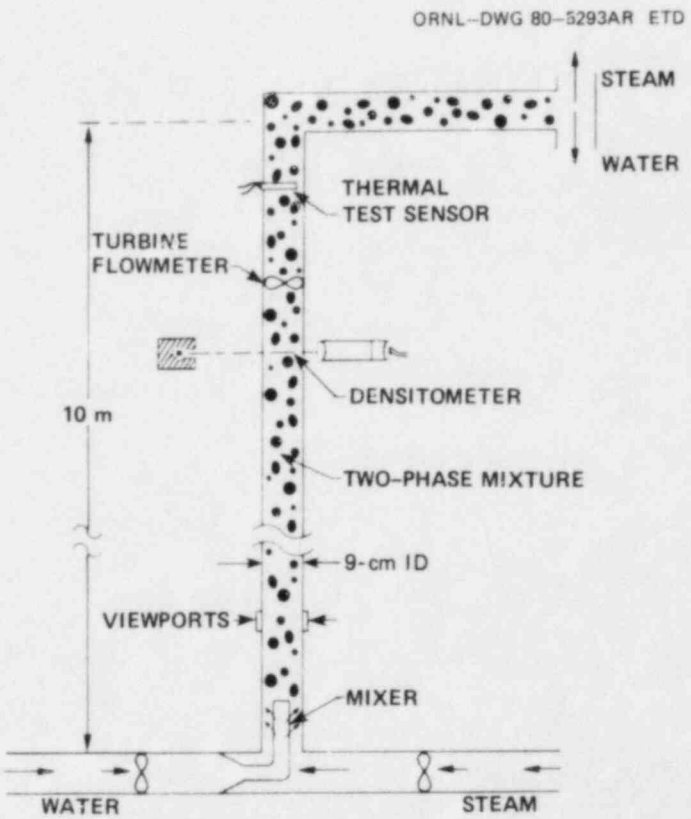

Fig. 3.6. Forced-convection steam/water test facility (AIRS Test Stand) used for thermal sensor evaluation at low and moderate pressures.

4 to 12 MPa (600 to 1750 psia). During testing, heater rod temperatures reached ~800°C (1500°F).

The THTF was operated by the PWR Blowdown Heat Transfer Program to obtain rod bundle heat transfer data requested by the USNRC. (A detailed description of the THTF may be found in Ref. 4.)

ORNL-DWG 81-1600 ETD

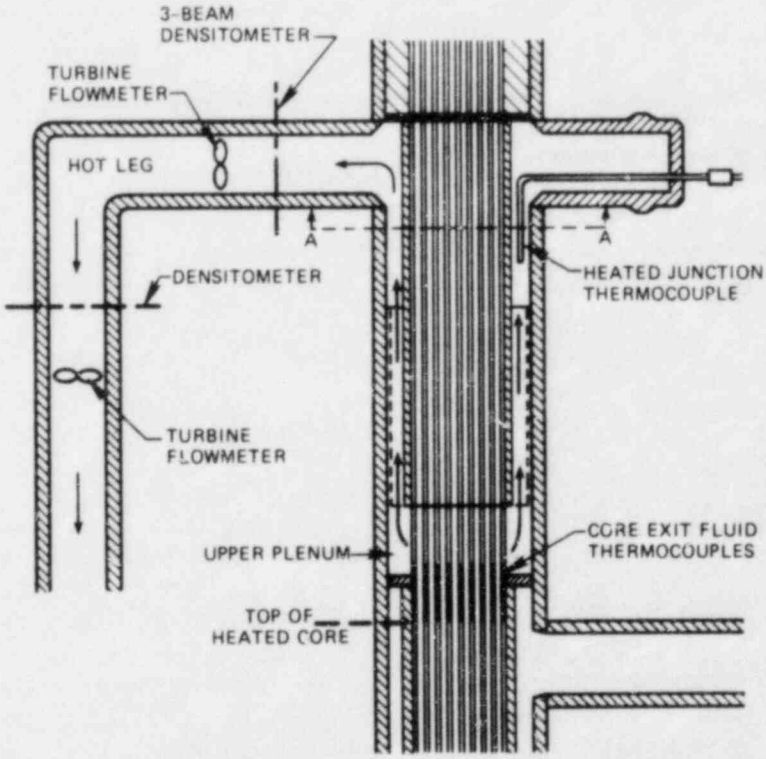

(a)

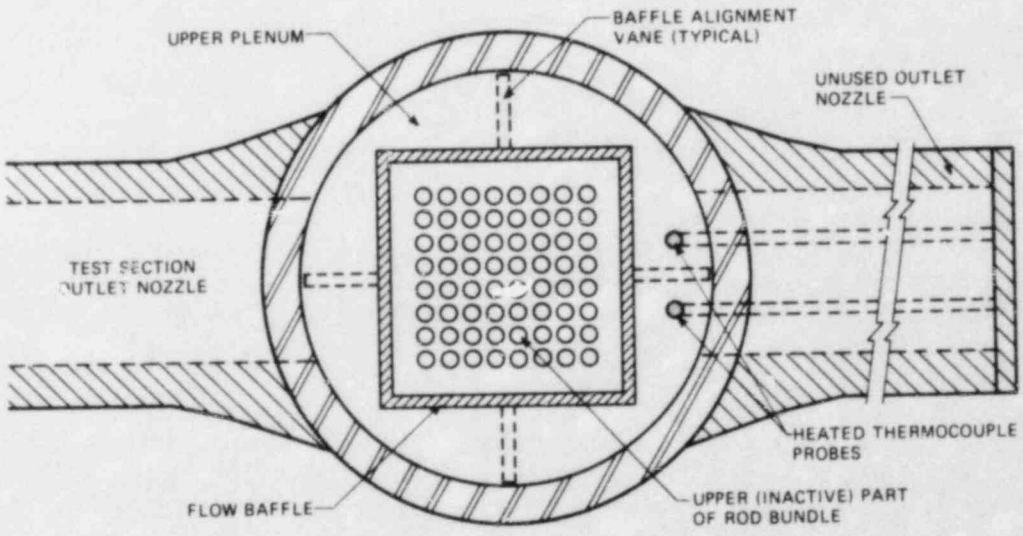

(b)

Fig. 3.7. (a) Schematic of upper part of THTF test section and outlet piping showing locations of HTC and other instrumentation and (b) cross-sectional view of THTF at plane A-A.

4. EXPERIMENTAL RESULTS

Experimental data are presented for thermal coolant sensors in a variety of test facilities and under several different operating modes. These data were accumulated from natural-circulation tests, forced-convection tests, special effects tests, and various HTC-control circuit tests.

Data will be shown first from the different control circuits, then from the natural-circulation and forced-convection tests, and finally from the special effects experiments.

4.1 Control Circuit Testing

Several methods are feasible for heating, controlling, and monitoring thermal coolant sensors. Some of these methods were investigated at ORNL.

Two primary methods for monitoring the heated sensors are to (1) connect the sensor differentially, thus negating system temperature changes; and (2) wire each thermal sensor separately, noting the difference between heated and unheated points. The second method can be used to monitor the fluid temperature by using the unheated junction sensor.

The heater can be powered in two general ways. The first and probably most common is by supplying a dc power input. There are two variations of this mode of operation: (1) maintain constant heater power and measure the resulting temperature rise; or (2) use the thermal sensor output to feed a controller to keep the thermal sensor at a set temperature, and measure the heater current. (Decreasing the surface heat transfer by immersing the sensor in vapor will decrease the heater current.) This method provides a self-protecting feature for the heater when the sensor has prolonged exposure to vapor. The second way of powering a thermal coolant device is by pulsed heater input. By pulsing the heater current, a periodic output signal can be generated. To determine if the sensor is immersed in liquid, one can either measure the rise time to a preset level (e.g., 63%), or the magnitude of the maximum electromotive force (emf). The principle advantage of the pulsed mode is that Ac detection techniques can be used (i.e., signal averaging and lock-in detectors). However, these detection techniques require a sensor with a relatively fast time response.

The curve in Fig. 4.1 shows the results of using constant heater power with an HTC level detector. A dip of 5°C occurred as the probe uncovered, presumably caused by evaporation of the water film remaining on the probe. Temperature of the HTC increased about 8.5°C and stabilized. Covering the device with water decreased the temperature of the HTC by 13.5°C. The ambient temperature in the pressurizer was changing with time; this caused the temperature changes between covered and uncovered states to vary. This experiment showed that even with modest constant heat input (~1 W), the HTC gave an indication of liquid level. A second test was run using the emf output of a differential TC connected to a three-mode proportional controller. A block diagram of the measuring equipment is shown in Fig. 4.2. Figure 4.3 shows a run made near room temperature with an HTC in the heater voltage indication mode. Lowering

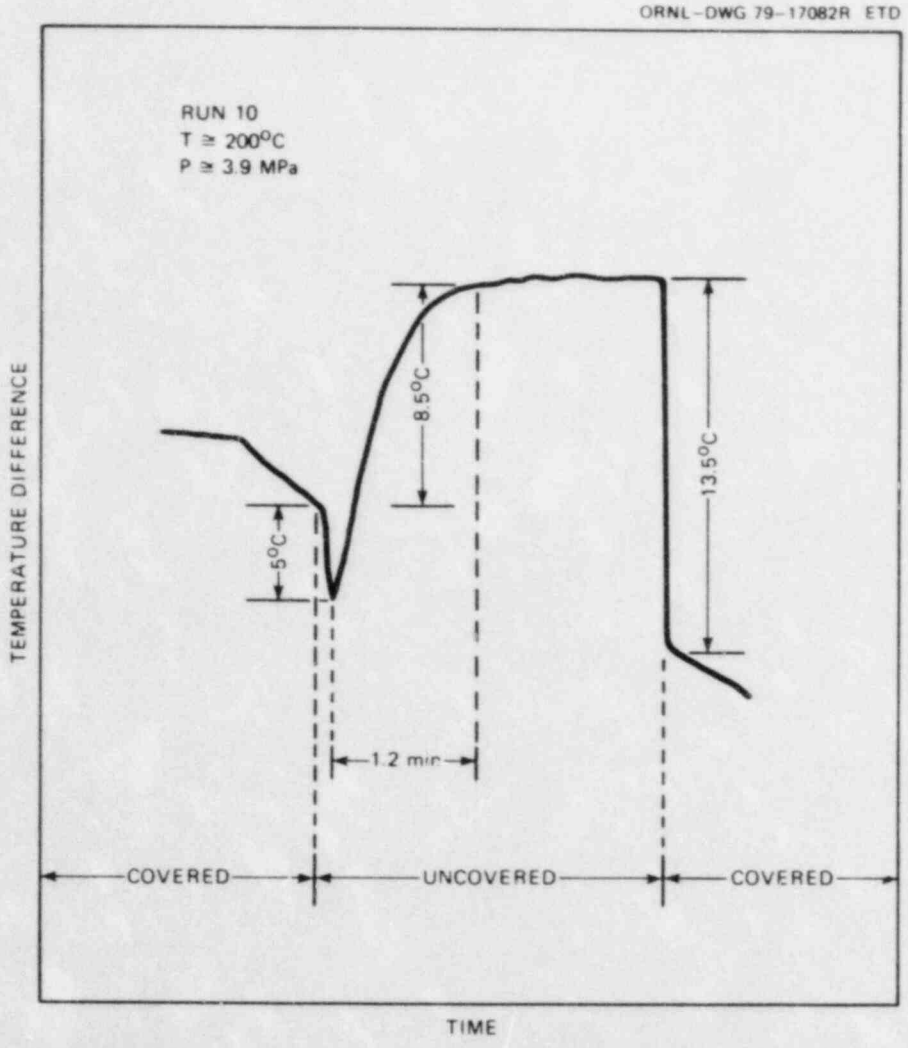

Fig. 4.1. Experimental results with prototype HTC level detector with constant heater power.

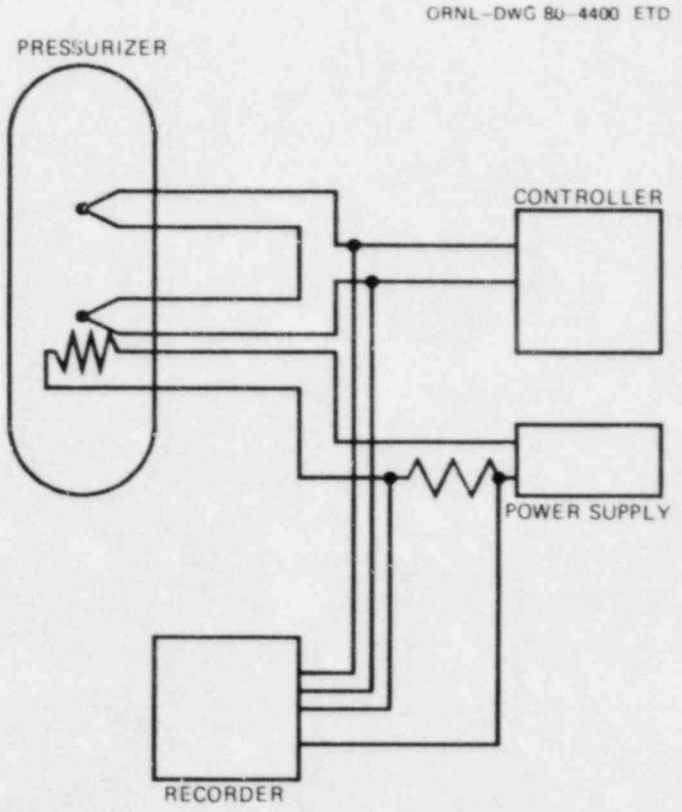

Fig. 4.2. Block diagram of measurement apparatus used in controlled ΔT mode.

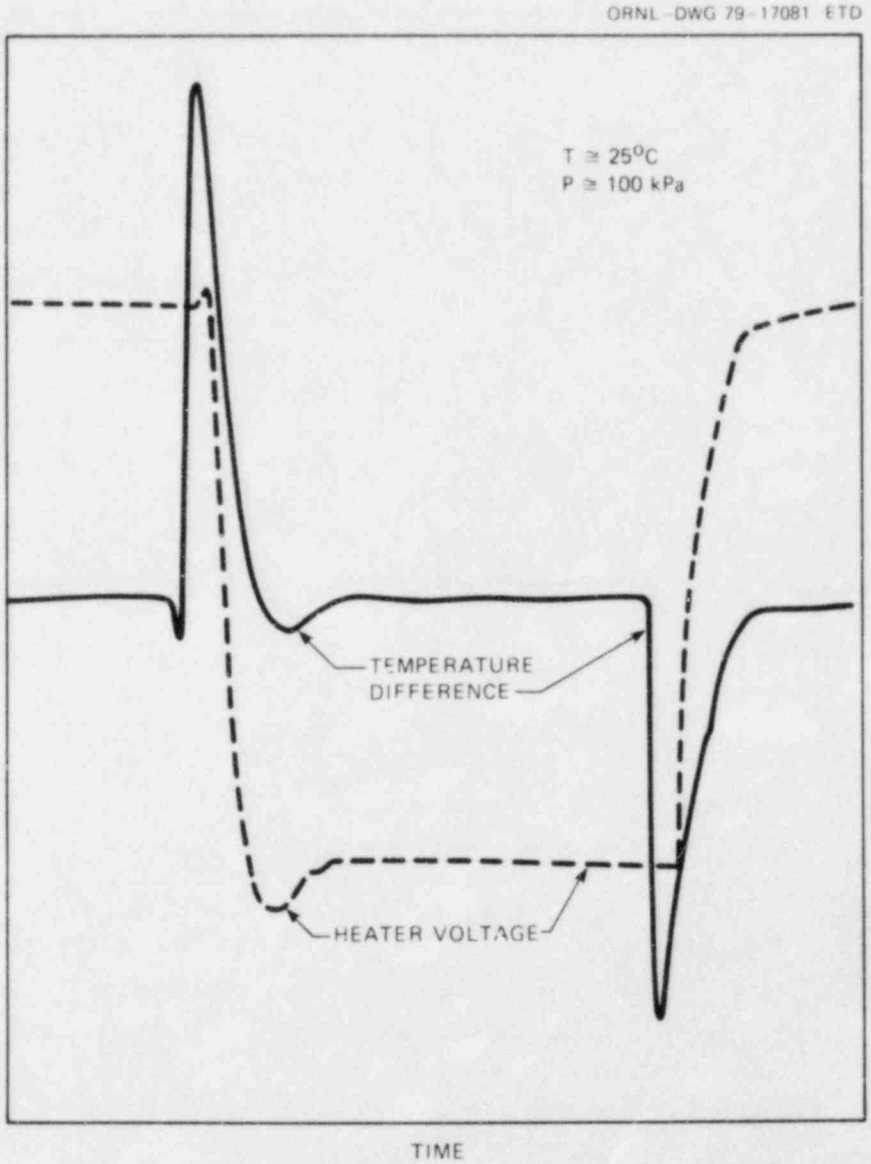

Fig. 4.3. Test of HTC with proportional controller to maintain constant ΔT. Solid curve is ΔT; dashed curve is voltage across heater.

the liquid level below the probe gave a clear 4-V drop in the heater voltage (Fig. 4.3). When the device was covered again, heater voltage returned to its original value.

One scheme using the pulsed heater technique is to use ordinary TCs (no separate heater) as sensors and heat the TC wires by an ac current. The TC emf was read using a filtered circuit. A schematic of this system is shown in Fig. 4.4. A blocking capacitor is placed in the output of the Variac to prevent the dc emf from the TC from being shorted through the windings of the Variac. The TC emf is filtered to remove the ac, buffered, and may be displayed on a meter. A test of the ac HTC probe was performed using a container of water at room temperature. Figure 4.5 is

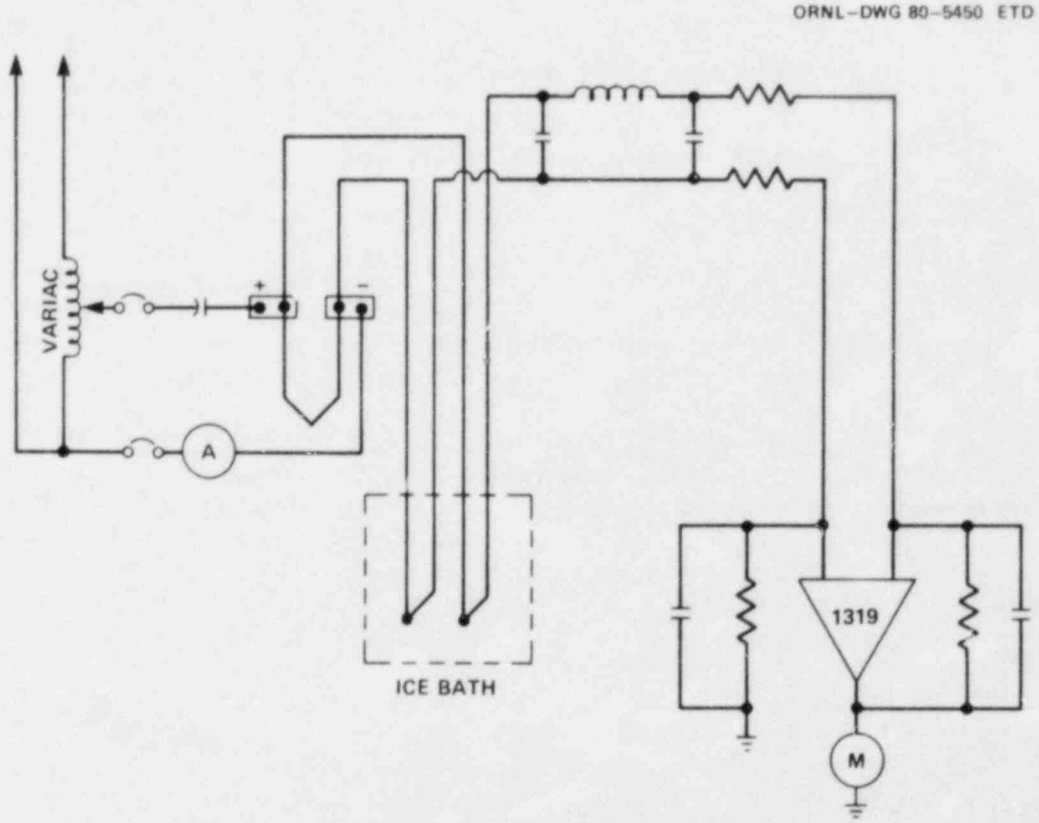

Fig. 4.4. Schematic of system used for self-heating tests of K-type TCs as liquid level sensors.

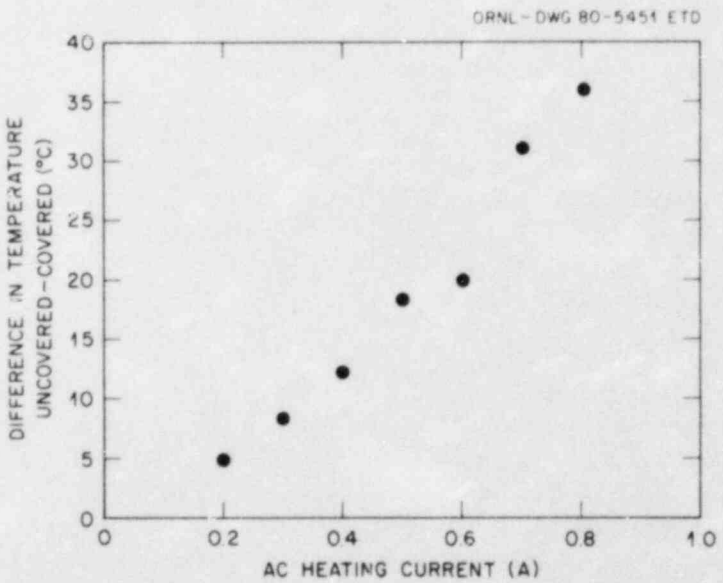

Fig. 4.5. Difference between covered and uncovered TC output recorded in room-temperature self-heating tests and plotted vs ac heating current.

a plot of the difference in indicated temperature between the covered and uncovered states vs the ac heating current. These data indicate that this method to detect liquid level can be used in cases where TCs are in contact with the fluid. Successful application may require some prior knowledge of the temperature rise in the covered and uncovered states in the particular location where the TC is installed. This method may be useful as a diagnostic tool, and the instrumentation should be relatively inexpensive.

The final method investigated at ORNL, the loop-current-step-response, is based on the fact that the time response of a TC sensor is strongly influenced by the heat conduction of the surrounding medium. In this method, a current is passed through the TC wires with a consequent temperature rise of several degrees centigrade. Decay of this temperature with time is recorded when the heating current is turned off. The time constant of the sensor can be determined from the shape of the temperature decay curves and is directly related to the thermal conduction between the sensor and its surroundings. When the sensor is immersed in liquid with a relatively high thermal conductivity, decay of temperature is more rapid than when it is immersed in vapor with only a fraction of the thermal conductivity of the liquid.

A loop-current-step-response apparatus was developed at ORNL for in situ testing of installed thermocouples, for example, in a nuclear reactor. A series of tests were conducted with the loop-current-step-response apparatus to determine if the method would be suitable for in-core liquid level detection using the available core TCs. Some results of these experiments are shown in the oscillographs in Fig. 4.6. At room temperature and pressure [Fig. 4.6(a)], a clearly discernible difference was seen between the time response of a liquid-covered probe and the probe immersed in vapor. At 200°C [Fig. 4.6(b)], the difference between the time response of the two media cases was not as great but was clearly detectable. Restrictions of the power supply in the present loop-current-step-response apparatus limited the temperature rise in the 3-mm-diam TC to ~2°C.

A disadvantage of this measurement scheme is that experience in the High-Flux Isotope Reactor (HFIR) at ORNL has shown that TCs developed an anomolous transient when the heating current was turned on or off after ~1000 h in the radiation capsule.[5] Under steady-state conditions, however, the TCs behaved normally, so that it appears that the pulsed mode of operation would not be viable after a few thousand hours. (A 1,000-h exposure in the HFIR would be roughly equivalent to 10,000 h in a typical power reactor).

4.2 Natural-Circulation Tests

This section contains the experimental results from natural-circulation tests in the Steam/Water Pressurizer. Tests were conducted from ambient pressure and temperature to 10.8 MPa (1545 psia) and 315°C (600°F). The level sensors were covered and uncovered with saturated water. An independent measurement of the liquid level in the pressurizer was obtained by using a ΔP transducer. The ΔP transducer was calibrated and

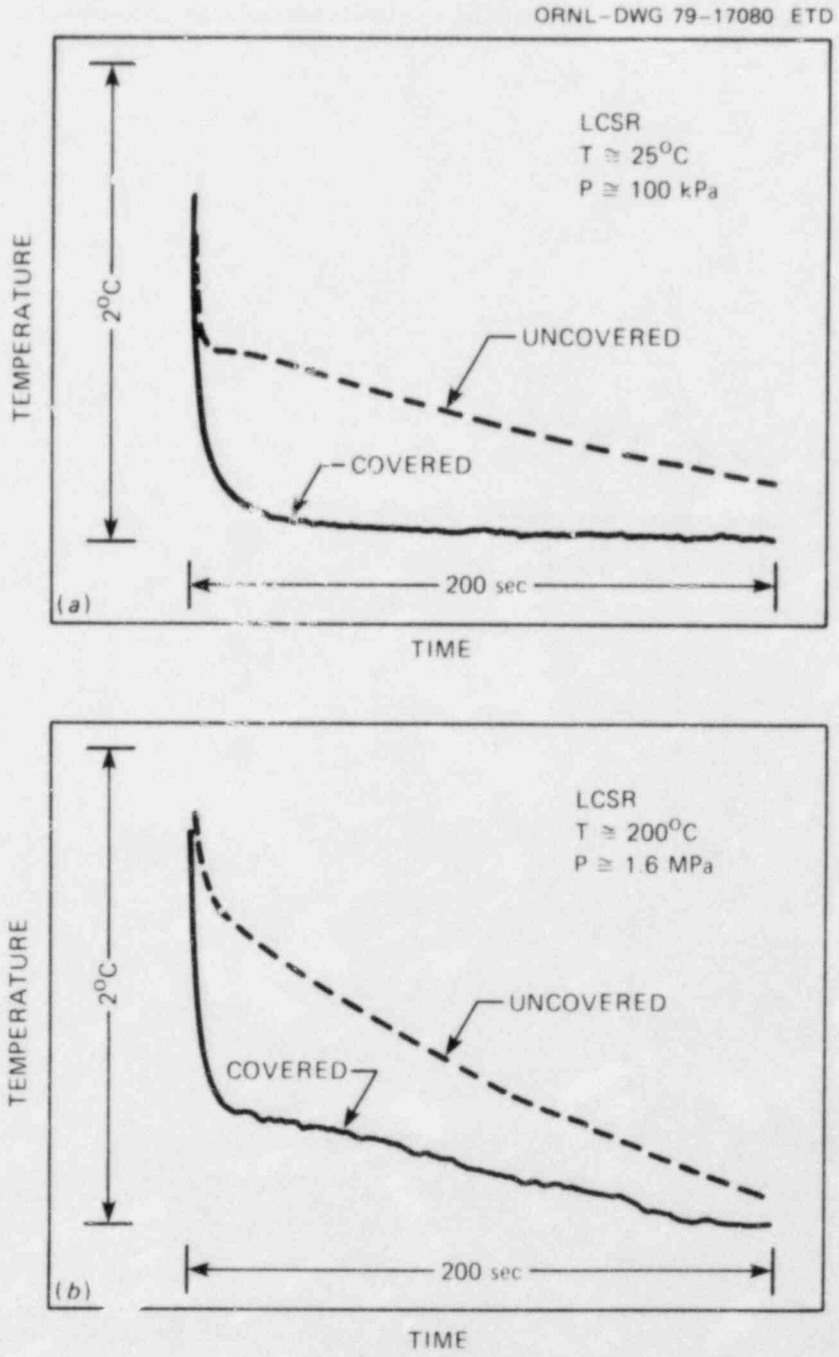

Fig. 4.6. Oscillographs obtained from loop-current-step-response test in TITF of normal 3-mm-diam TC as liquid level sensor. For all traces, full-scale temperature (vertical) axis is ~2°C; full-scale time (horizontal) axis is 200 s. (a) Data recorded at room temperature; (b) data recorded at 200°C.

corrections for density changes were made when used at elevated temperatures and pressures. Also, at the higher pressures the effect of the steam density was accounted for in level calculations.

4.2.1 ORNL-designed HTCs

An HTC, ORNL I, was tested in the pressurizer. For each test point, a constant dc power was supplied to the 6.5-Ω probe heater. Differential TC output voltages were obtained with heater currents ranging from 350 to 1600 mA. Four series of tests were conducted with three locations of the HTC probe along a (horizontal) radius of the pressurizer, about halfway from top to bottom of the vessel (Fig. 4.7). The ranges of data taken during the test series are indicated in Table 4.1. A digital voltmeter and a continuous chart recorder were used to record the output signal of the differential TC during testing. Figure 4.8 shows the recorded ΔTs obtained during these test series. Each graph includes data for a particular pressure and temperature range. Each data point represents a mean ΔT reading obtained after the TC output was judged to have reached a steady-state value.

Table 4.1. Test matrix with ORNL HTC 1

Test series	Date of test[a]	Distance[b] (cm)	Heater current range (mA)	Pressure range (MPa)
1	1/14	5.0	63–500	0.1–10.2
2	1/15	0.2	115–750	0.1–1.5
3	1/16	0.8	400–750	0.1–3.6
4	2/5–6	0.8	400–1640	0.1–4.2

[a] Testing took place in 1980.

[b] Distance between probe tip and vessel wall.

Data show that at a given heater current the steady-state ΔTs recorded when the test sensor was immersed in saturated steam were always greater than the ΔTs recorded when the probe was covered with liquid. The sequence of plots at successively higher ambient pressures and temperatures shows that changes in ΔT from covered to uncovered states decrease with increasing pressure. This is largely caused by the improvement in natural-convection heat transfer to saturated steam at higher steam pressures and densities.

The variation in recorded ΔTs from run to run may be caused by the change in location of the probe with respect to a structure inside the vessel (Fig. 4.7) that formed a cover or hood over part of the HTC. The

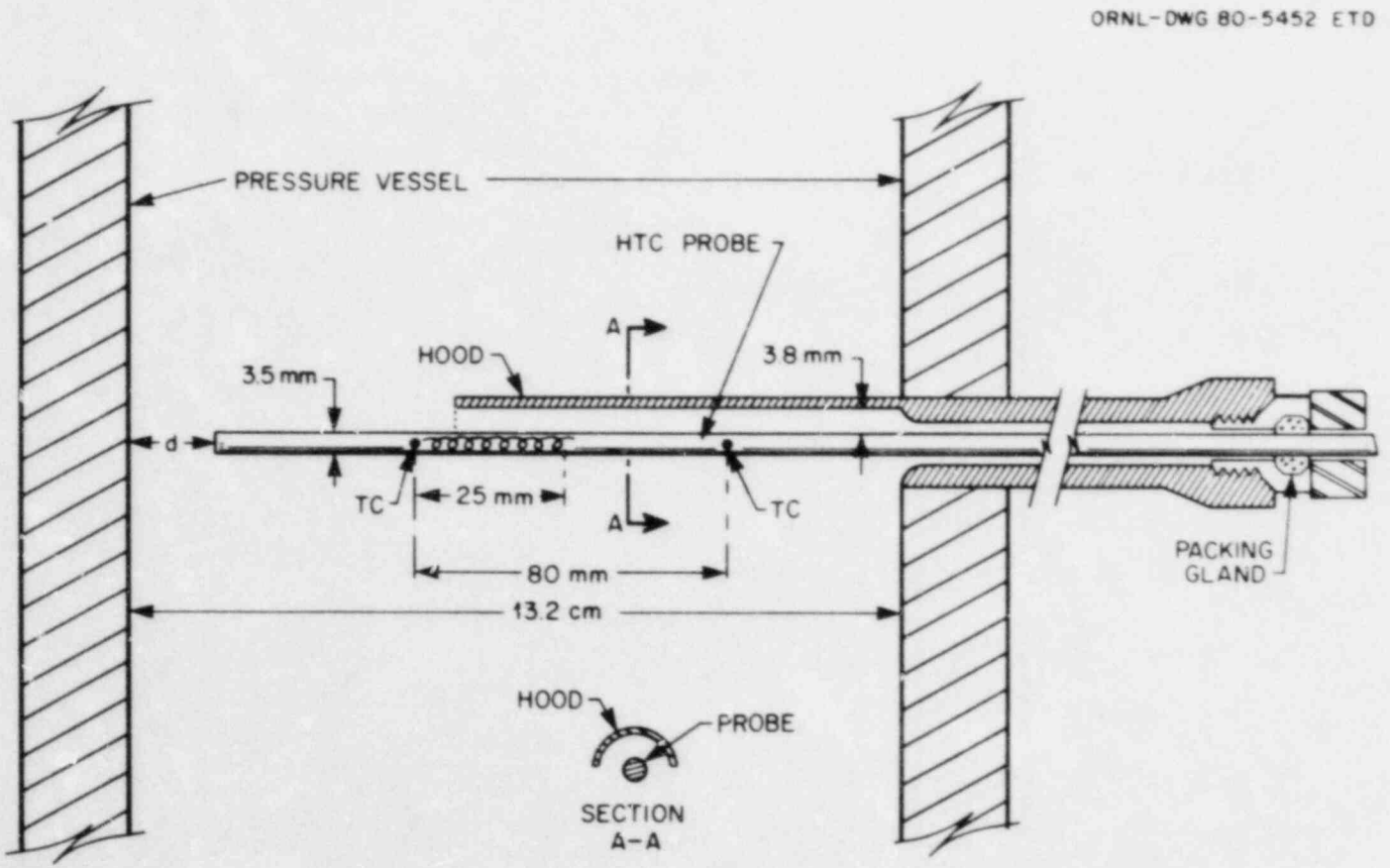

Fig. 4.7. Schematic showing location of HTC sensor ORNL I in TITF pressurizer for natural-convection experiments.

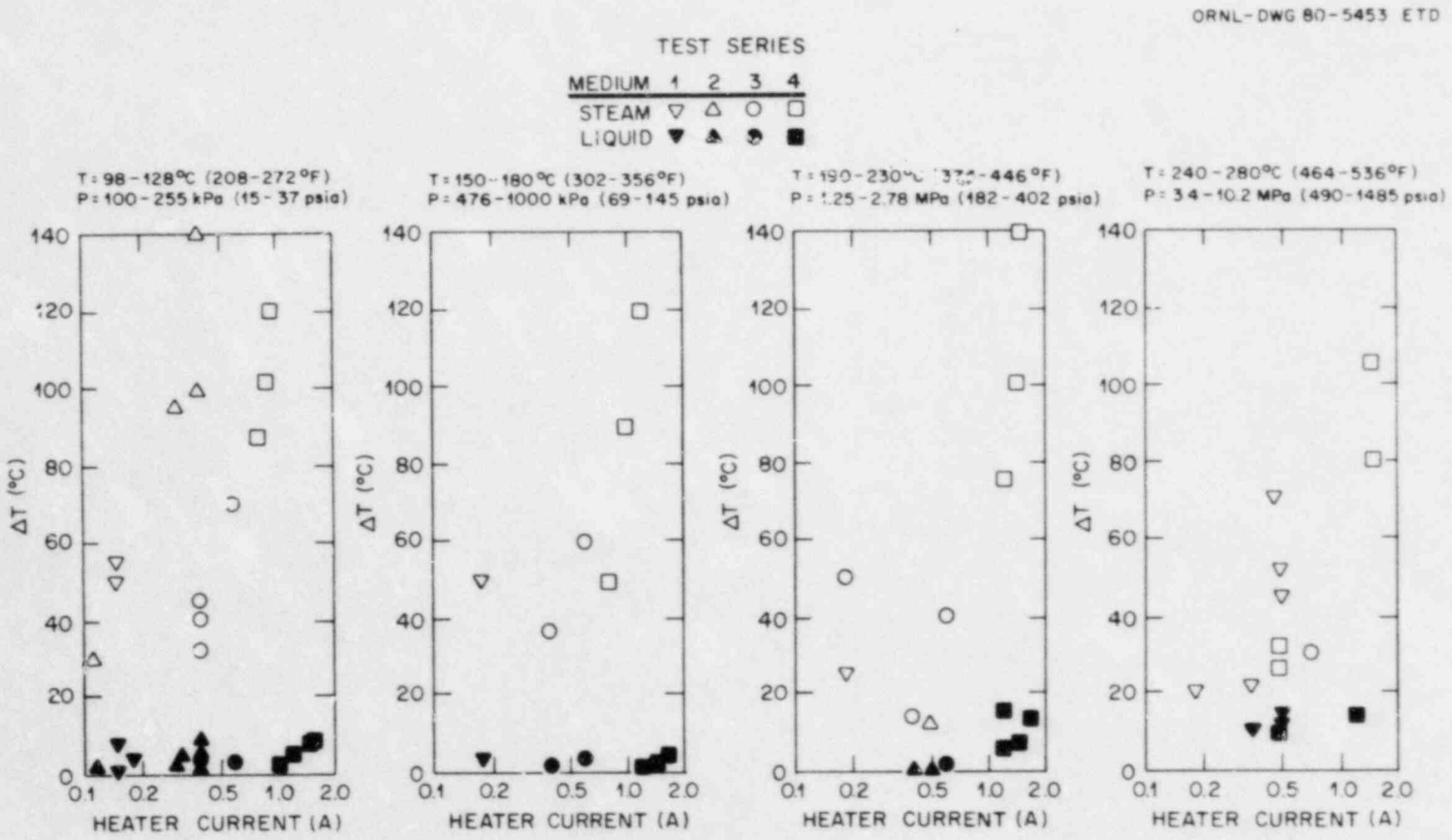

Fig. 4.8. Mean ΔT derived from TC output in TITF pressurizer test with HTC ORNL I and plotted vs heater current.

hood was part of the pressurizer assembly itself installed when the pressurizer was used with another facility; the hood was removed for later tests.

Additional tests were needed to establish repeatability of probe performance, particularly at pressures >3.4 MPa (500 psia). An improvement in probe performance was expected with the removal of the internal structures in the vicinity of the probe.

An example of the sensor time response observed during these tests is shown in Fig. 4.9. During the test period heater power was 1.0 W, corresponding to a local surface heat flux of 0.35 W/cm² (0.11 Btu/h·ft²). The curve indicates that, after the probe was uncovered, ~70 s were required for ΔT to reach 63% of its maximum. On recovering the probe, <2 s were required for the output temperature to fall to 37% of maximum ΔT.

A second series of experiments were run with the test sensor (ORNL I) in the pressurizer after the hood that covered the probe during the first series of tests was removed. As before, for each test point a constant dc voltage was applied to the 6.5-Ω probe heater. Differential TC output voltages were obtained with heater currents ranging from 400 to 2800 mA. A digital voltmeter and a continuous chart recorder were used to record the output signal during testing. [The OD of this probe was 3.5 mm (0.14 in.), and its heated length was 2.5 cm (1 in.). At the maximum heater current of 2.8 A, the steady-state surface heat flux, assuming no axial

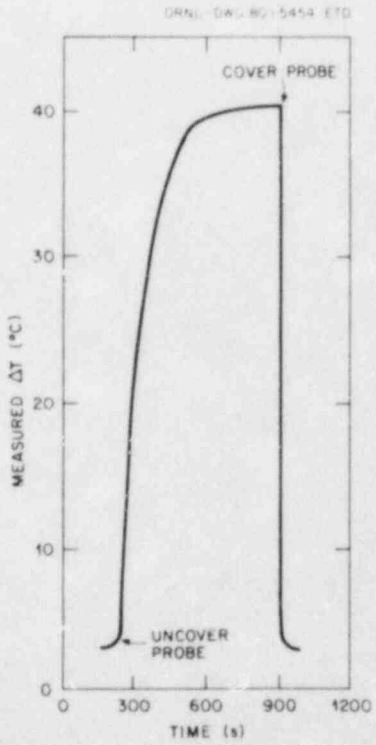

Fig. 4.9. Transient response of HTC ORNL I recorded during test series 3: heater power = 1.0 W, temperature in vessel = 100°C, pressure in vessel = 100 kPa.

conduction, would be ~18 W/cm² (116 W/in.²). This exceeds the steady-state surface heat flux of ~13 W/cm² (80 W/in.²) from a 1.0-cm-diam nuclear fuel pin at maximum decay heat power levels.]

Figure 4.10 shows the ΔTs recorded from the ORNL I HTC as a function of heater power with system pressure (at saturated conditions) and surrounding medium (liquid or vapor) as parameters. Each data point represents a mean ΔT reading obtained after the TC output reached a steady-state value.

At a given heater current, the data show that steady-state ΔTs recorded when the test sensor was immersed in saturated steam were always greater than ΔTs recorded when the probe was covered with liquid. The sequence of curves at successively higher ambient pressures and temperatures shows that ΔT decreases from covered to uncovered states with increasing pressure. The decrease is largely caused by the improvement in natural-

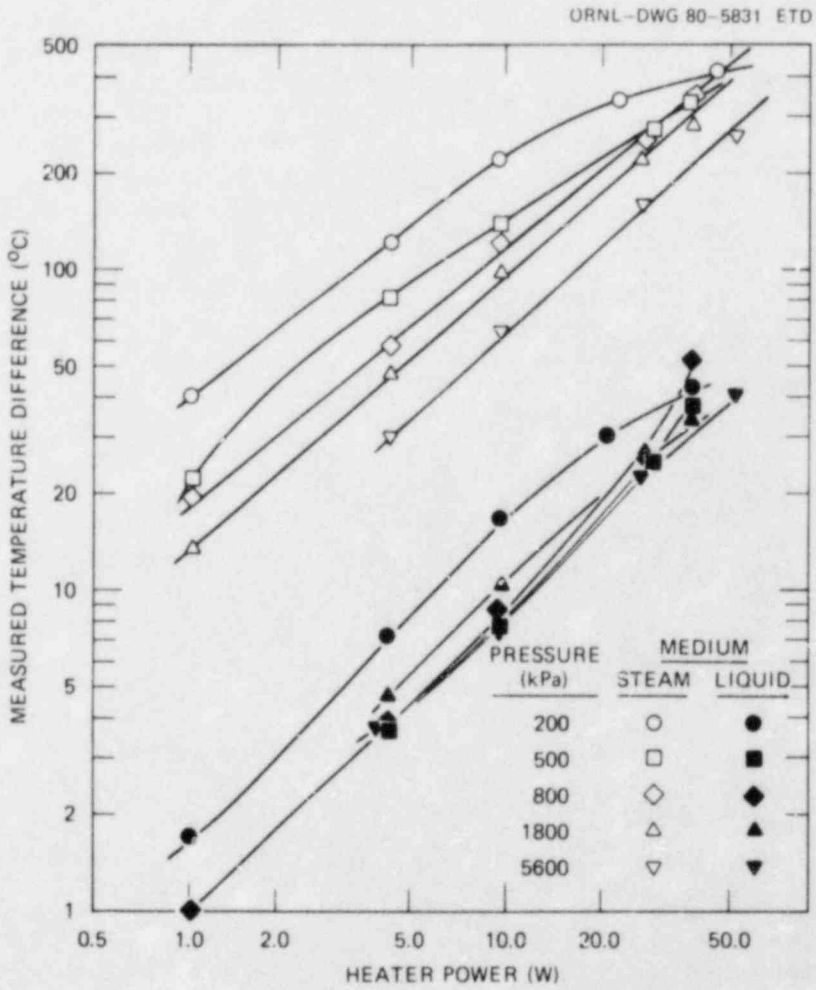

Fig. 4.10. Steady-state ΔTs recorded from HTC probe ORNL I in natural convection to saturated steam and water. Data are plotted vs power produced in probe heater with system pressure and medium surrounding probe as parameters.

convection heat transfer to saturated steam at higher steam pressures and densities.

The ΔTs recorded by the differential HTC are not an accurate measurement of the ΔT between the probe surface and the bulk fluid. There are at least two reasons for this. (1) Axial heat conduction along the probe, particularly when the surface heat transfer coefficient is low, may heat the reference junction and reduce the ΔT. [The decrease in slope of the ΔT vs power curve at ΔTs above 300°C (Fig. 4.10) is probably caused by this effect.] (2) With a high surface heat transfer coefficient, there may be a relatively large ΔT between the centerline of the probe under the heater where the HTC junction is located, and the probe's surface temperature. Thus, differential output from such a probe may indicate the order of magnitude of the surface heat transfer coefficient but may not determine it accurately. (This is not a criterion for ICC devices.)

With the hood removed from the pressurizer, the variations observed in ΔTs from run to run were reduced. Condensate from the hood may have been falling on the sensor, cooling the heated junction, and causing the deviations.

Figure 4.11 includes steady-state output ΔTs obtained as a function of heater power and system pressure (at saturation conditions) for two series of tests. The agreement between the two runs for the uncovered (dry) state is good. A general decrease in the output ΔTs was recorded in the covered state in the latest run compared with the earlier one. This change may be caused by the addition of a second probe sheath, which was installed to protect the probe internals from water. [The original probe sheath had been damaged by compaction of the sealing material in compression fittings (used to seal the probe in the pressurizer)].

4.2.2 Navy-type HTC

The Navy-type HTC was also tested in the pressurizer. Mounted vertically in the pressurizer, the probe was enclosed in a single sheath with heated and reference TC junctions separated axially by 18 cm. The HTC junction was nearer the probe tip and lower in elevation than the reference junction. The probe diameter at the heater was 3.7 mm, and the heated length was 1.0 cm. The measured ΔT was recorded with the sensor covered with saturated water or steam, with heater powers ranging from 0.4 to 21 W and system temperatures ranging from 25 to 300°C.

Steady-state response curves for the Navy HTC probe are shown in Fig. 4.12. Methods of probe operation and data interpretation for the natural-convection tests were like those used with the ORNL probe, as previously described. Again, a distinct difference in probe output existed, depending on whether the probe was immersed in liquid or vapor. A particular state (covered or uncovered) was defined such that all of the probe's heated portion was immersed in that phase. Negligible change in probe output occurred as the liquid level rose from just above the heater past the reference junction.

A decrease in output ΔT with increasing ambient pressure and temperature was again observed for the vapor state (Fig. 4.12). The ΔT curves obtained in the covered state show less dependence on pressure than do the vapor curves, but the reduction of observed ΔT at constant heater power

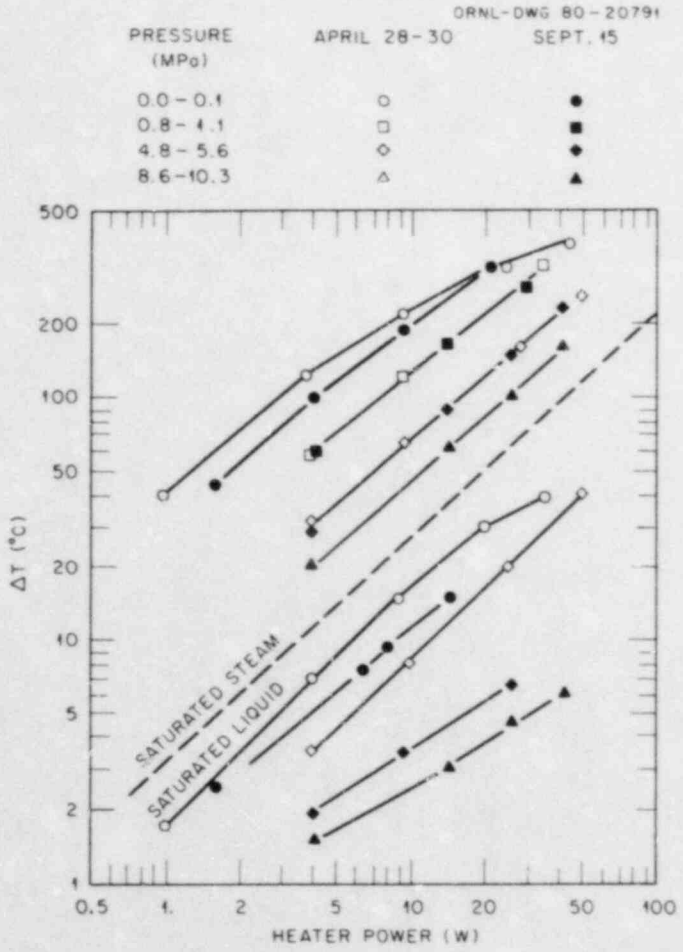

Fig. 4.11. ΔTs recorded from HTC probe ORNL I in natural convection to saturated steam and water, plotted vs power produced in probe heater. Individual data points represent steady-state ΔTs obtained when probe was immersed in saturated steam and water (see legend).

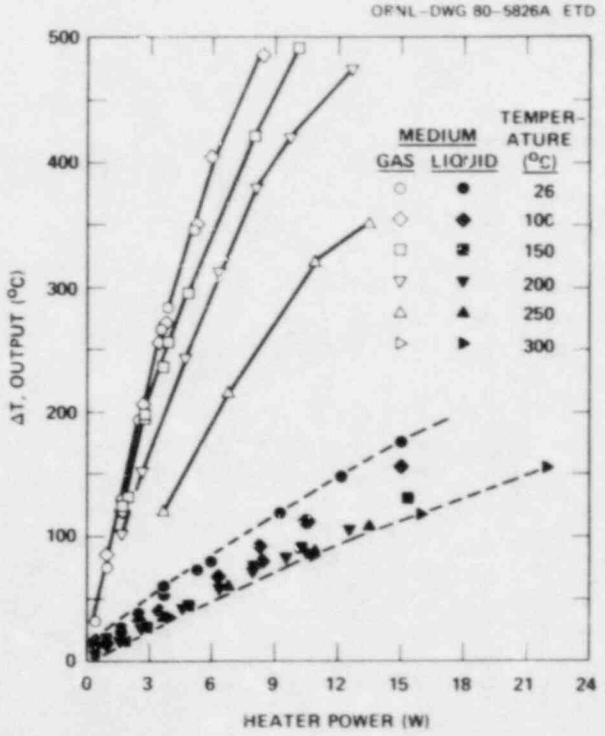

Fig. 4.12. Steady-state ΔTs recorded from Navy-type HTC sensor in natural convection to steam and water. Data are plotted vs power produced in probe heater with system temperature and medium surrounding probe as parameters.

and increasing pressure is in agreement with trends predicted by a widely used nucleate boiling heat transfer correlation.[6] However, a large variation existed in output ΔT while the probe was uncovered (Fig. 4.13). [The uncovered ΔTs (Fig. 4.12) represent the maximum ΔT observed at a given uncovered condition; this value was found to be fairly repeatable.] Figure 4.13 shows a ΔT output from this probe plotted vs time, while the ambient pressure and temperature were 1.6 MPa and ~200°C, respectively. The

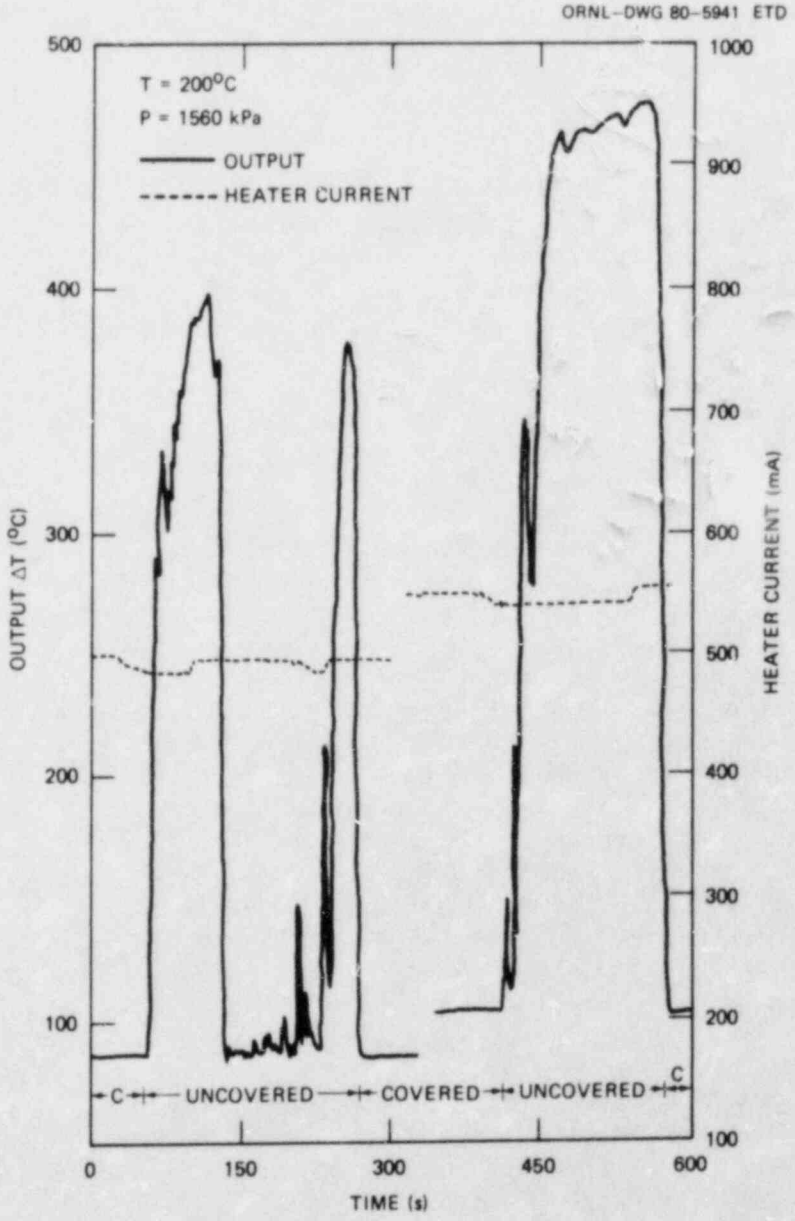

Fig. 4.13. Navy-type HTC output recorded vs time during natural-convection tests at 200°C. Heater current ranged from ~500 to 550 mA. During period denoted as covered, active part of probe was immersed in saturated liquid. During uncovered period, probe was immersed in saturated steam.

temperature decrease from 400 to ~90°C with subsequent reheating to ~375°C is believed to be caused by a period of rewetting of the probe's heated region by condensate. The upper part of the TITF pressurizer was not heated during these tests and condensation on internal surfaces probably did occur. Subsequent tests with the Navy probe oriented vertically in the transparent countercurrent steam-water test facility showed that this type of rewet behavior did indeed occur with a vertically oriented probe.

The conclusion based on these results is that if a probe of this type is to indicate degraded cooling conditions reliably in the presence of a high void fraction environment, some provision must be made to protect the probe's heated region from droplets and condensate.

4.2.3 Heated resistance temperature detectors

Two thermal-type liquid-level-interface monitors with resistive thermometers connected differentially were installed in the pressurizer and tested under high-temperature and -pressure conditions. The instruments were purchased from Fluid Components, Inc.; one, Model FR-7766-HT, was 25 mm in diameter and the other was a miniaturized version, which was 10 mm in diameter.

The 25-mm HRTD sensor was installed horizontally along a radius of the pressure vessel. The sensor head was positioned ~3 cm from the vessel centerline; the plane of the sensor elements was horizontal. The vendor-supplied control unit provided a constant power level of ~2 W to the probe heater.

Tests were conducted with the HRTD at saturated conditions from 100 to 300°C (212 to 572°F) with pressures from 100 to 820 kPa (15 to 1190 psia). When the probe was immersed in saturated liquid, its output was always <10 mV. Steady-state output voltages obtained when the probe was in saturated steam are plotted vs system pressure in Fig 4.14. The decrease of the output ΔT with increasing pressure reflects the increase in natural-convection heat transfer coefficient with increasing pressure. However, even at the highest pressures (and temperatures) the output voltage from the HRTD between liquid and vapor is different by an order of magnitude (~100 mV in vapor, <10 mV in liquid).

Unsteady output temperatures were again observed with the HRTD when the sensor head was in saturated steam. The effects were most pronounced at the highest pressures, for example, the output signals at 300°C shown in Fig. 4.15(a). The exact mechanism for these effects is not understood. However, at the recommendation of the probe manufacturer, a half cylinder was added to the sensor head to shield the head from water drops that might fall on the sensor. Results obtained after this modification were greatly improved [Fig. 4.15(b)], indicating that falling drops did cause the variation observed in the unshielded probe output.

The miniaturized HRTD was functionally the same as the larger model except for a much smaller OD, 1.0 cm (0.4 in.).

The HRTD was tested under the conditions listed in Table 4.2; output voltages obtained after the probe reached steady state in saturated steam are also given.

These data are similar to those obtained with the larger (25-mm-diam) HRTD. When the probe was immersed in saturated liquid, the steady-state

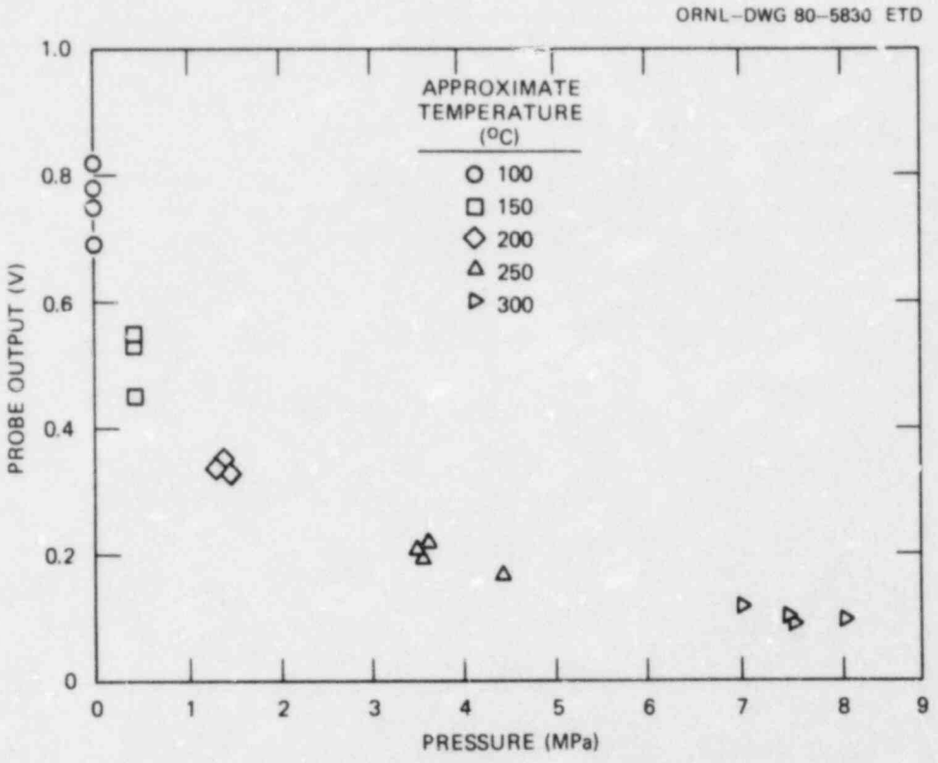

Fig. 4.14. Steady-state output, obtained from heated RTD device when sensor head was immersed in saturated steam, plotted vs system pressure.

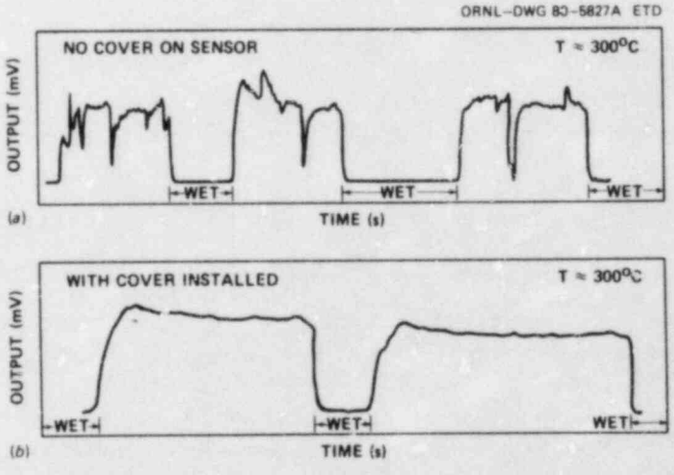

Fig. 4.15. Time-dependent output obtained from heated RTD device during natural-convection experiments performed at ~300°C (pressure ~8.6 MPa). (a) Data obtained with bare sensor head as shown in Fig. 4.14, (b) data obtained while sensor head covered as described in text.

Table 4.2. High-temperature and -pressure test of 1-cm-diam heated resistance temperature detector sensor

Ambient conditions		Medium		Sensor head output (mV)
Temperature (°C)	Pressure (MPa)	Liquid	Vapor	
101	0.2	X		-6.1
99	0.1		X	56.0
154	0.4	X		-6.3
143	0.4		X	54.0
190	1.2	X		-6.0
186	1.1		X	50.6
273	5.5	X		-7.3
266	4 8		X	36.3
314	10.1	X		-8.0
305	8.6		X	22.5

output voltages were <5 mV. A constant heater power was used throughout the test. On uncovering the sensor, the time required for output voltage to increase to 63% of its asymptotic value was ~6 s; little effect of ambient pressure or temperature on the response time was noticed. Also, with the vertical sensor orientation, no apparent problems with spurious rewetting of the sensor occurred. The cylindrical end cap provided was an adequate splash shield for the heated elements in the natural-convection tests.

4.2.4 Multiple-position HTC arrays

To use discrete thermal-type sensors to trend liquid levels will require a vertical array of sensors. Previous tests of HTCs and HRTDs at ORNL have used single sensors only. Two multiple-position-type HTCs were fabricated and tested under high-temperature and -pressure conditions. The primary goal of these tests was to evaluate probe design for a probe assembly in a single sheath containing multiple heaters and thermal sensors.

The three-element array was built and tested in the Steam/Water Pressurizer. The active portion of the HTC array was installed through a hole in the top of the vessel. The 2.5-cm-long heaters were centered at 51, 66, and 81 cm below the vessel top. Liquid level in the vessel was also determined using ΔP measurements. A four-element unheated TC array was installed parallel to the HTC assembly and used to measure liquid-vapor temperatures during the vessel fill and drain operations.

Time response of the three heated sensors may be characterized by 1/e-folding time of the absolute temperature signal in response to application or removal of heater power or to changing liquid level. The former method

is more representative of the probe itself. Typical values for the 1/e-time response of the HTC array were found to be ~35 s.

Preliminary data reduction was performed by calculating

$$\hat{h}_i = \frac{I^2}{\Delta T_i} ,$$

where I was the total probe heater current, and ΔT_i was the measured ΔT between a heated and an unheated TC. In each TC pair used for a ΔT, the heated junction was physically above the unheated TC junction. At a given system pressure, the liquid level was raised and lowered over the probe active region. The ΔT for a particular TC pair was found to vary little after that pair was relatively far from the liquid-vapor interface. In Fig. 4.16, values of $\hat{h}_i$ are plotted vs system pressure for the three TC

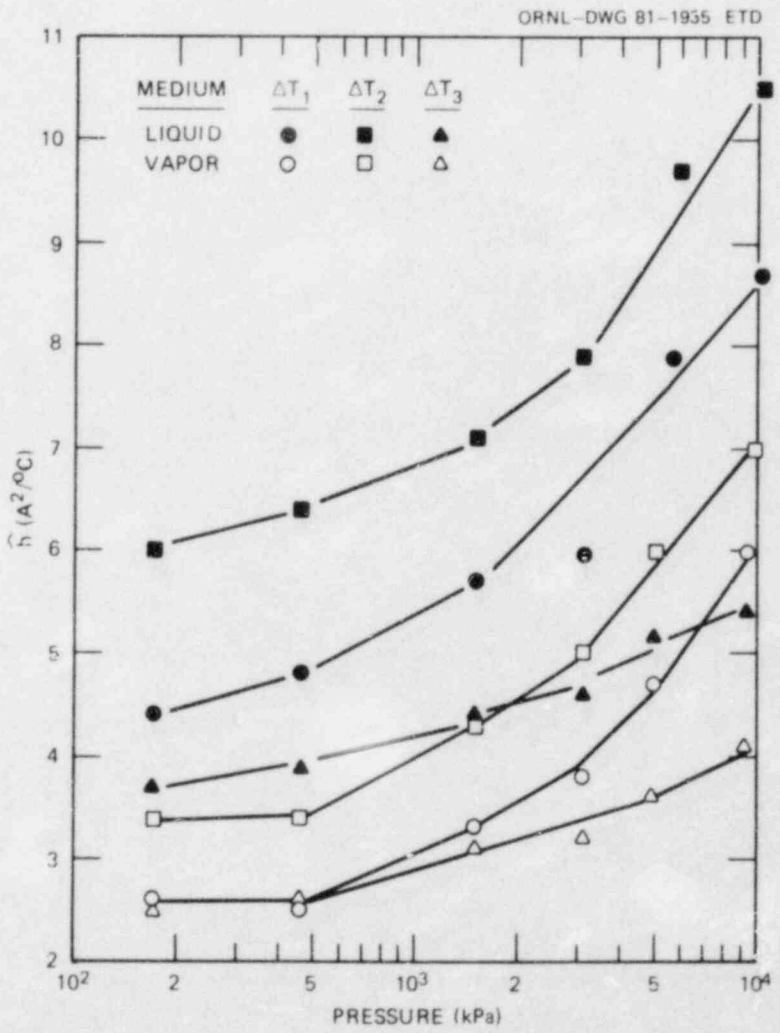

Fig. 4.16. Steady-state values of h_i (see text) for each HTC pair as a function of system pressure and medium (liquid water or steam).

pairs in the test probe and for the covered and uncovered states. The graph shows that $\hat{h}_i$ increases with increasing pressure for every TC pair and state. Significant individual differences among various pairs are evident. However, $\hat{h}_i$ was at least 30% higher in the covered state than in the uncovered state for all TC pairs throughout the pressure range tested.

The probe conducted significant amounts of heat from the heated region in an axial direction, particularly when the heated zone was uncovered. This conduction caused two effects: (1) heating of the reference junction by adjacent heaters and (2) loss of resolution in detecting liquid level while in the vicinity of the heater. Tests of the same probe assembly at room temperature revealed a similar "washing out" of the signal level.

The second MPHJTC was installed in the pressurizer (Fig. 4.17), and experiments were conducted at three pressures and temperatures. This

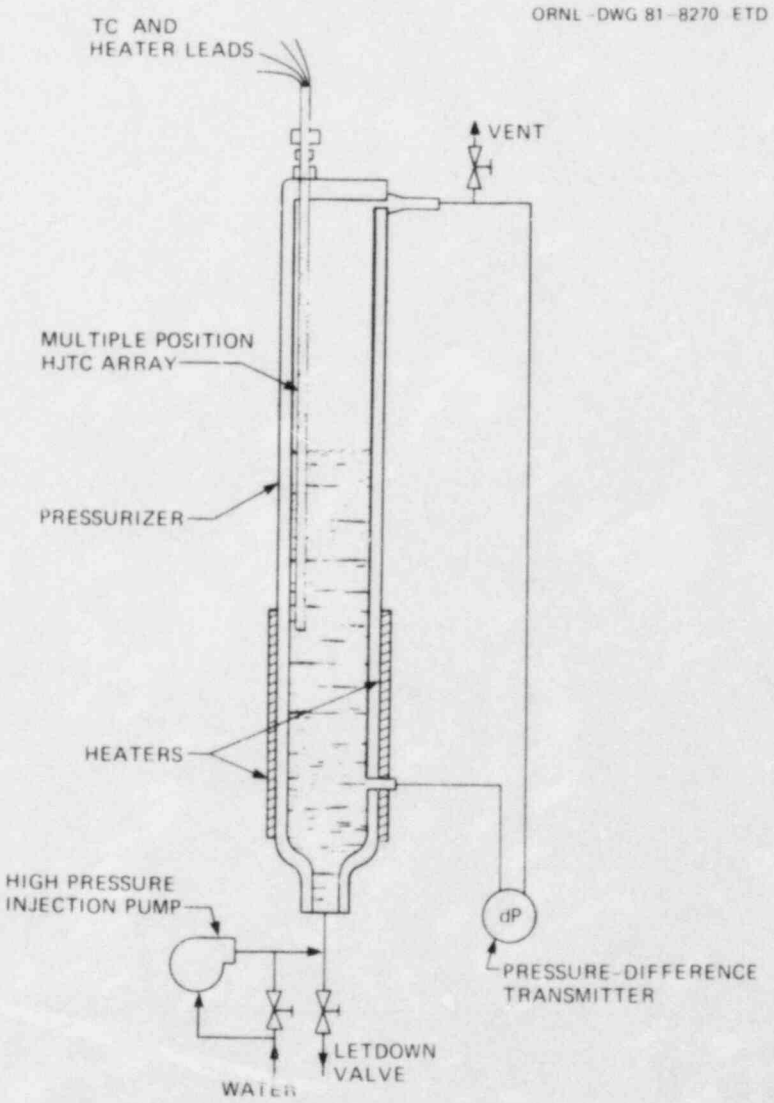

Fig. 4.17. MPHJTC array location in the pressurizer.

probe was swaged to increase its density and reduce axial heat conduction. Table 4.3 lists the fluid conditions and power settings for the MPHJTC for each of the three experiments. For the ambient pressure and temperature test, the pressurizer was filled with water, and the power to the heaters was adjusted to yield a 4 to 5°C difference between the heated and unheated TC pair. The loop water level was slowly dropped (~1.5 cm/min) while the eight TC outputs were monitored along with a ΔP cell. The ΔP cell (Fig. 4.17) was calibrated just prior to testing. When a noticeable increase in temperature of a TC was observed, the corresponding ΔP cell reading was recorded. The draining process continued until all eight TCs were uncovered. The higher pressure tests were conducted in a similar manner. Table 4.4 lists results of the testing and reveals an easily discernible ΔT between water-only and steam-only data. A plot of liquid levels predicted by the MPHJTC and the ΔP measurement for ambient conditions is shown in Fig. 4.18. Excellent agreement between the ΔP measurement and MPHJTC level was found at all eight locations. (A small ΔT was noted at the unheated TC when the level passed; this gives four heated and four unheated locations.) Good agreement was noted at the higher pressures

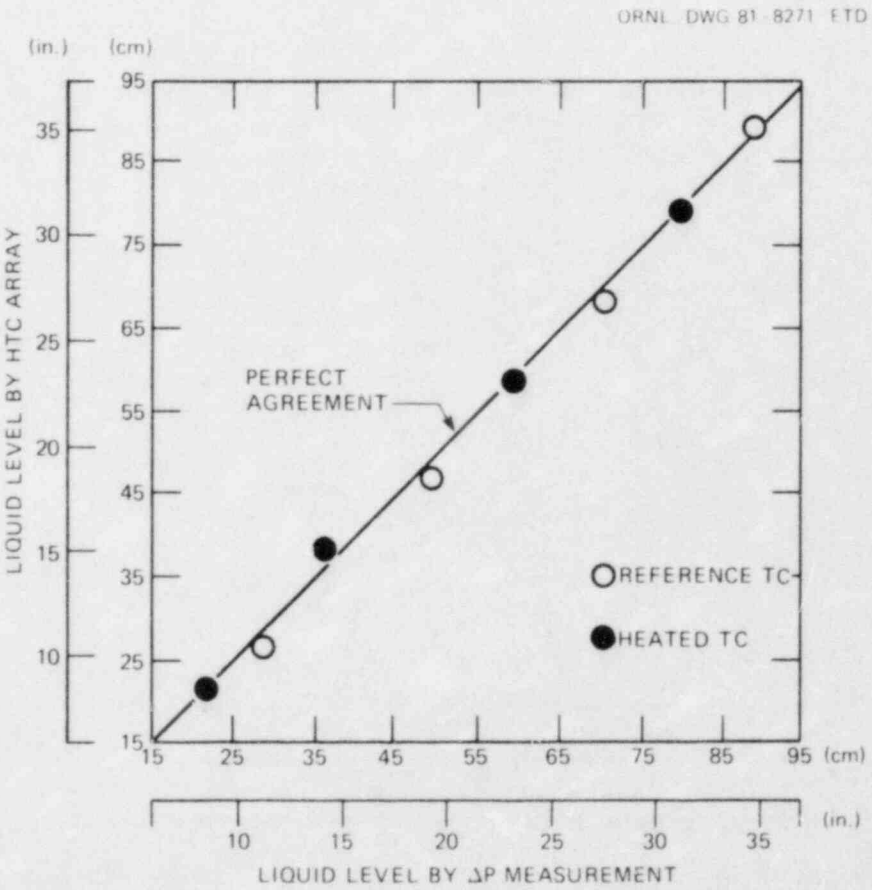

Fig. 4.18. MPHJTC array liquid level test results at ambient temperature and pressure.

Table 4.3. Fluid conditions and power settings for MPHJTC natural-convection tests in the pressurizer

Test No.	System pressure[a] (MPa)	System temperature (°C)	Voltage supply (V)	Heater current (A)	Power[b] (W/heater)
1	0.10	28	4.9	2.3	2.8
2	2.7	230	8.0	3.45	6.9
3	10.8	315	9.5	4.0	9.5

[a] 1 MPa = 145 psia.

[b] Four heaters in the device.

Table 4.4. Results of natural-convection tests with the MPHJTC in steam and water

Test No.	System pressure[a] (MPa)	System temperature (°C)	Thermocouple heater position[b]	Temperature difference (°C)	
				Water	Steam
1	0.10	28	H-1	4.6	48
			H-2	4.8	49
			H-3	4.7	48
			H-4	5.0	59
2	2.7	230	H-1	1.6	42
			H-2	2.2	62
			H-3	2.1	[c]
			H-4	[c]	[c]
3	10.8	315	H-1	1.0	50
			H-2	1.9	38
			H-3	1.7	46
			H-4	[c]	54

[a] 1 MPa = 145 psia.

[b] H-1 is top thermocouple pair in pressurizer; H-4 is bottom thermocouple pair.

[c] Data not recorded.

with somewhat more scatter because of uncertainties in the ΔP cell measurement (temperature and pressure corrections to the water density). The heated thermocouple array was able to distinguish liquid level to approximately ±1.9 cm at ambient pressure and ~6.4 cm at pressures up to 10.8 MPa (1545 psia). Axial heat conduction was significantly reduced for this sensor as compared with the previous three-element probe.

4.3 Forced-Convection Tests

Experiments to evaluate the performance of thermal-type coolant sensors under forced-convection conditions were performed in (1) the low-pressure Steam/Water Flow Visualization Loop, (2) the AIRS test stand, (3) the 3-Mod A/W IDL, and (4) the THTF. The tests in the THTF were under LOCA conditions.

4.3.1 Low- and intermediate-pressure tests

The Navy-type HTC and the probe designated ORNL I were tested in the flow visualization loop (Fig. 3.5). The ORNL probe was installed horizontally ~2 cm above the tie plate. The Navy probe was vertically oriented with the heater ~25 cm above the tie plate. Data obtained with both probes in single-phase liquid flow and single-phase steam were generally similar to those obtained in natural-convection tests: the ΔTs obtained in steam flow were much greater than those in liquid flow.

In two-phase flow with widely varying void fractions, the output ΔTs for both ORNL and Navy probes remained virtually identical to the values observed when the flow was single-phase liquid. This effect held true even when visual observations revealed that relatively little of the liquid phase was present near the probe. (No in situ void fraction measurements were made during these tests.)

In an attempt to quantify the observations obtained from the flow visualization loop testing, the Navy and ORNL probes were installed in a horizontal orientation in the AIRS test stand (Fig. 3.6). Tests were performed at system pressures of 380, 520, and 725 kPa (55, 75, and 105 psia). Data plotted in Fig. 4.19 show the output ΔT as a function of measured density and heater power. The data indicate that the probe output is virtually independent of velocity and void fraction down to very low densities. When the flow consisted of only saturated or superheated steam (no liquid phase), the probe output increased significantly.

Heater powers used in these tests resulted in probe surface heat fluxes of $\lesssim 9.10$ W/cm² (58.7 W/in.²). This figure is ~70% of the maximum decay heat surface heat flux from a typical nuclear fuel rod and ~3% of the maximum full power surface heat flux expected from such a pin.

Data from a thermal sensor were replotted in Fig. 4.20 with output ΔT as a function of flow quality. These data emphasize that HTCs indicate cooling capacity very nearly the same as single-phase liquid until very high void-high quality flow. This cooling phenomenon also occurred in heated rod bundle experiments (PWR-Blowdown Heat Transfer Program at ORNL). Rod surface temperatures remained low except at very high qualities (Fig. 4.21).

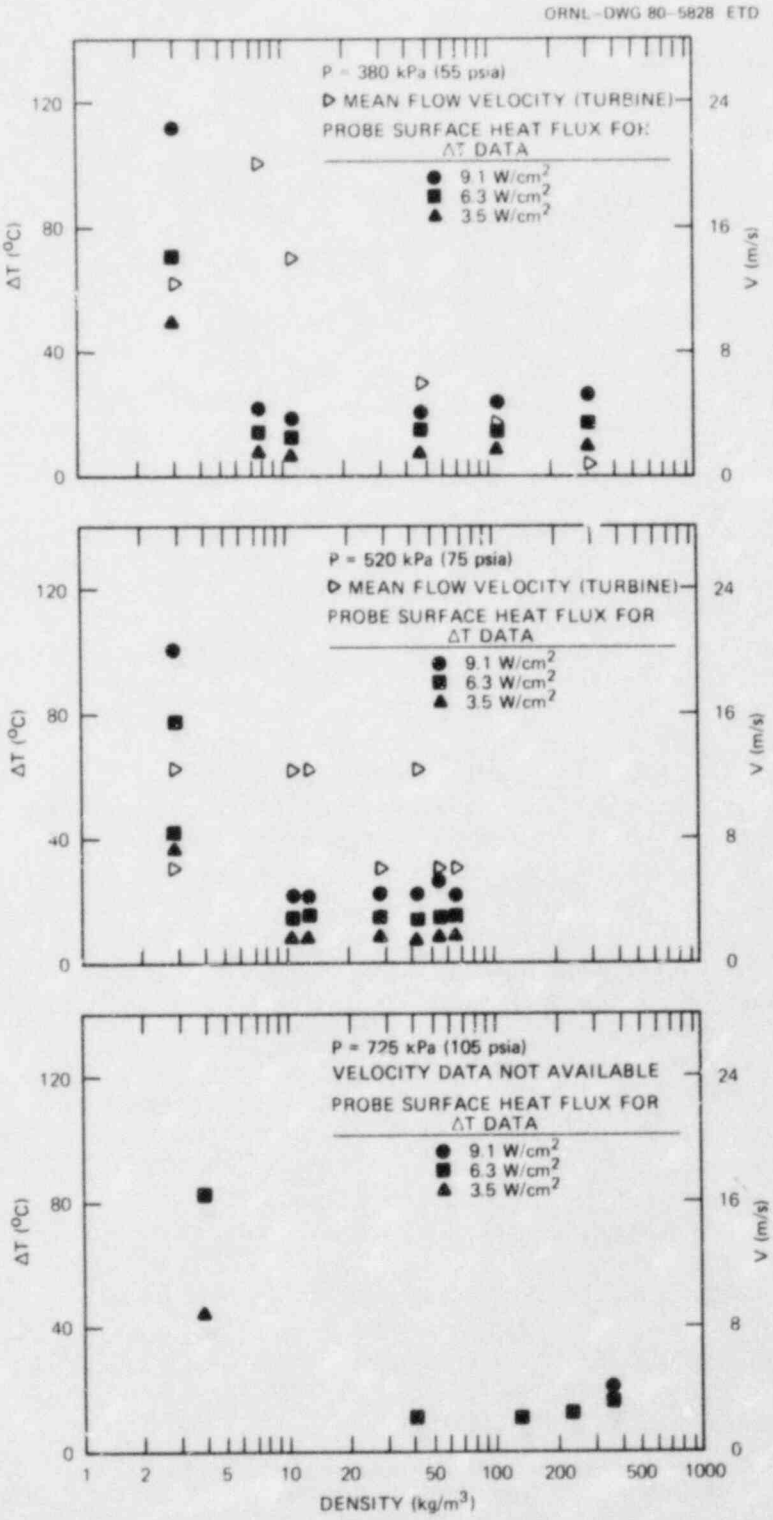

Fig. 4.19. ΔT data obtained at 380, 520, and 725 KPa with HTC sensor ORNL II in forced convection in AIRS Test Stand. Data are plotted vs density derived from densitometer readings. Flow velocities indicated by turbine and heater power are parameters.

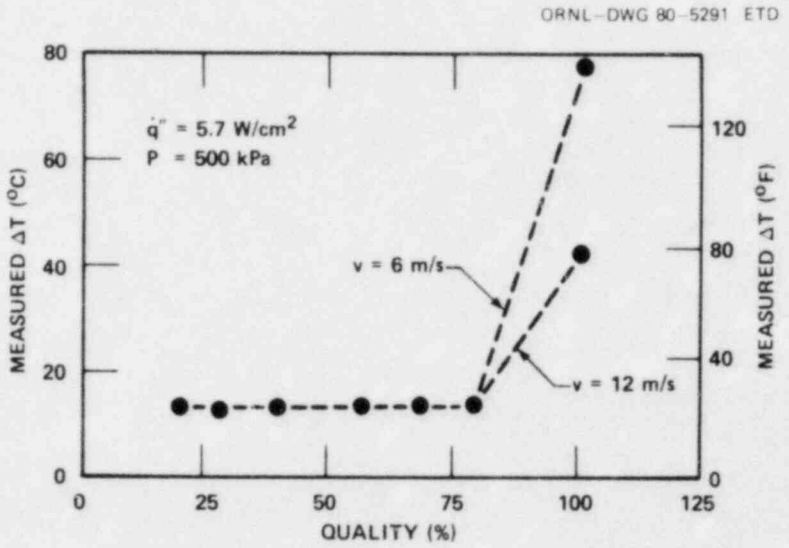

Fig. 4.20. Measured ΔT from HTC vs flow quality. ΔT also shown as function of flow velocity.

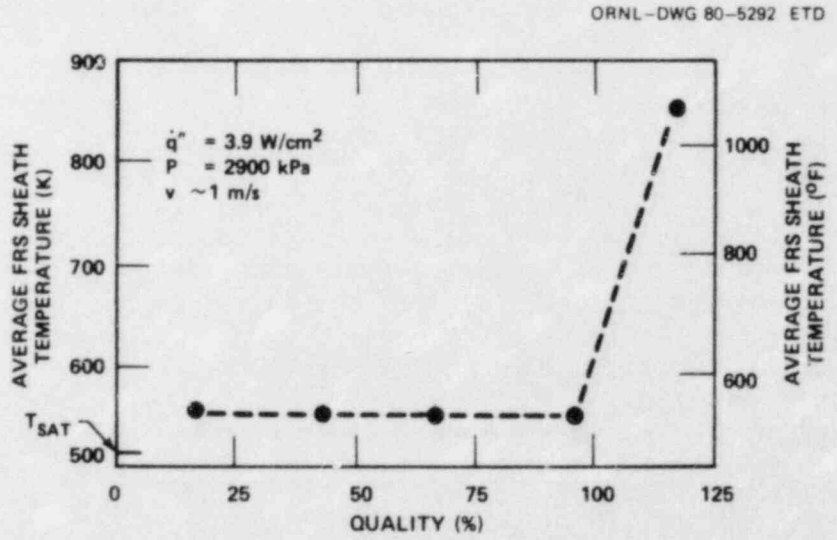

Fig. 4.21. Average FRS sheath temperature vs flow quality in THTF.

The tests performed in these forced-convection facilities clearly indicate that only a minimal amount of liquid is required to cool a thermal sensor, operating at decay heat power rates, to relatively low ΔT outputs. If HTC probes are to detect the approach to inadequate cooling conditions (particularly if they are to work in forced-convection high-void-fraction flow), the sensors must be shielded from the liquid phase present in the flow stream.

4.3.2 LOCA conditions tests

During the evaluation of coolant sensors for PWR vessel liquid level detection, many tests were performed in facilities where some aspect of the fluid conditions in a hypothetical LOCA was simulated. However, because such instruments are intended to give an indication of the cooling capacity of the reactor coolant system, the candidate devices were tested in conjunction with an LOCA heat transfer experiment. Particularly, the main criterion in evaluating the devices was the predictability of the test instrument's response to fluid conditions as the fluid interacted with a heated rod bundle. The THTF at ORNL was used to perform such testing.

An HTC provided by C-E was operated during two series of experiments: one series included film boiling and the second one included boiloff, uncovery, and reflood. The film boiling tests (THTF 3.07.9) were performed to obtain steady-state film boiling data under flow rates and bundle power conditions analogous to a small-break LOCA in a PWR.[7] The bundle boiloff, uncovery, and reflood experiments were performed to investigate high-pressure, low-flow steam cooling, and high-pressure reflood. These tests (THTF 3.09.10) are distinguished from THTF 3.07.9 by significantly lower bundle flow rates and power levels.

In both test series, the HTC was installed in the THTF upper plenum near the test section outlet nozzle [Fig. 3.7(a)]. The HTC's output was the differential voltage between the heated and unheated TCs. (C-E stated that their device represents a stage in their development program for reactor-vessel liquid level instrumentation and should not be considered their completed design. Other specific information regarding the probe and splash shield configuration are considered proprietary to C-E).

A manually controlled dc power supply was used to provide power to the probe heater. Applied voltages (and resulting probe currents) were chosen based on the system pressure as specified by the HTC supplier. Generally, higher voltages were used at higher THTF system pressures. Supplied with constant heater current for a given test point, the output ΔT of the HTC was monitored.

Film boiling tests were performed for the conditions shown in Table 4.5. For a given test condition, the system pressure and inlet flow rate of subcooled water were held essentially constant. Rod bundle heater power was increased to produce film boiling in the upper part of the rod bundle. Output ΔT of the HTC was monitored before, during, and after periods of film boiling in the rod bundle. The test objective was to relate the HTC response to rod bundle surface temperatures and to the fluid conditions at the test section outlet.

A typical set of data from the HTC, an outlet densitometer, and the turbine are shown in Fig. 4.22. These data are for a system pressure of

Table 4.5. Preliminary results summary from HTC in THTF during Test 3.07.9

System pressure[a] (MPa)	Rod bundle mass flux[b] (kg/s·m²)	Maximum test section outlet volume flow[c] (L/s)	Bundle thermocouple levels uncovered[d]	Maximum HTC output (mV)
4.3	255	54	F,G	9
6.2	230	70	F,G	12
6.2	363	88	F,G	12
6.2	407	70	F,G	16
6.2	524	70	F,G	13
8.7	230	72	F,G	13.5
9.2	382	98	F,G	12.0
8.5	505	153	F,G	0.5
8.3	647	164	F,G	2.1
8.3	804	175	F,G	0.5
12.4	211	23	G	19.6
12.4	309	68	E,F,G	14.8
12.4	461	91	E,F,G	3.8
12.4	573	91	E,F,G	2.5
12.4	696	118	D,E,F,G	2.3

[a] 1 MPa = 145 psia.

[b] 1 kg/s·m² = 735 lb_m/h·ft².

[c] 1 L/s = 15.9 gpm.

[d] Levels D, E, F, and G are 182.9, 124.5, 63.5, and 3.2 cm below top of heated length, respectively.

6.6 MPa (960 psia) and a test section mass flux of 230 kg/s·m² (50 lb/s·ft²). As the rod bundle power was increased during the period from 0 to 50 min, the output velocity increased while the measured density decreased. The HTC data exhibited spikes, probably caused by intermittent dryout and rewet, during the period 13 to ~40 min; during the same period, the outlet density decreased from ~640 to ~130 kg/m³ (~40 to ~8 lb/ft³). The HTC apparently dried out at 43 min at an outlet void fraction of 89%. Density data suggest that a significant amount of liquid was still present in the outlet flow during the period from 40 to 70 min. The HTC ΔT remained high, indicating poor cooling for ~25 min before the first rod bundle surface temperature excursion [departure from nucleate boiling (DNB)] was observed at 70 min. At 83 min, after the desired heat transfer data at those flow conditions were recorded, bundle inlet mass flow was increased, and the rod bundle and the HTC were quenched nearly simultaneously.

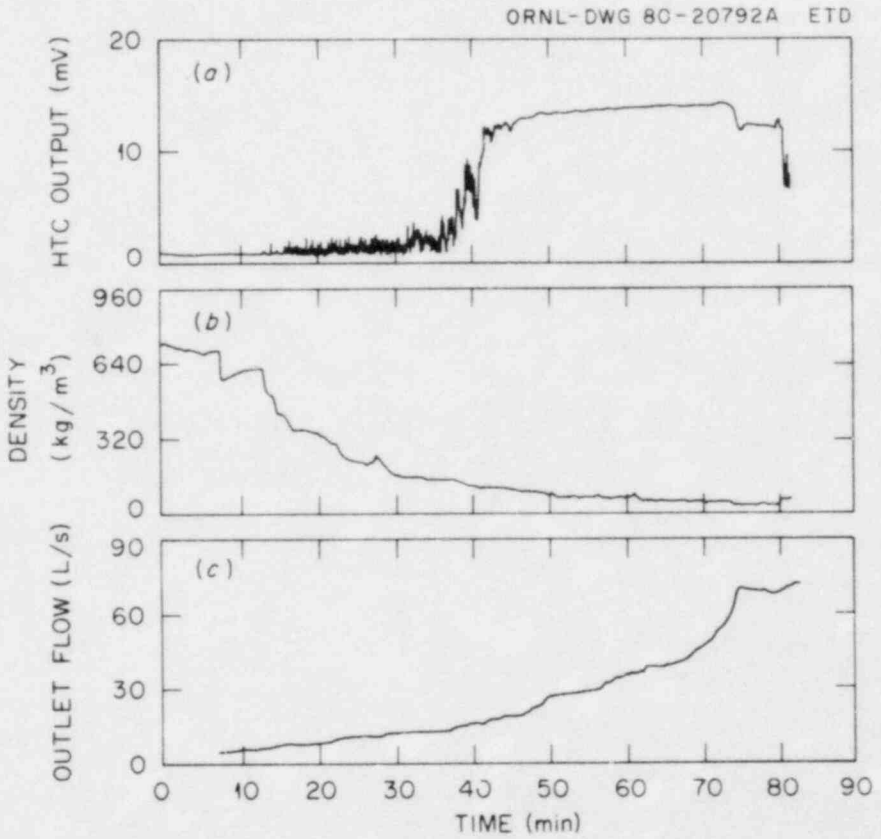

Fig. 4.22. Time response of HTC, outlet densitometer, and turbine flowmeter in THTF during part of Test 3.07.9. During period shown, system pressure ranged from 6.3 to 8.7 MPa (920 to 1260 psia). Rod bundle mass flux was ~230 kg/m²·s (169,000 lb_m/h·ft²).

This process was repeated many times to obtain data at the other conditions shown in Table 4.5. In most cases the HTC ΔT increased to ≥10 mV (~250°C) prior to onset of film boiling (rod surface flux exceeding critical heat flux) in the rod bundle. However, when the test section mass flux was ≥500 kg/s·m², the HTC output remained <4 mV (~100°C), even when parts of the rod bundle were in film boiling (Fig. 4.23). During those periods, the outlet turbine flowmeter indicated a velocity of at least 11 m/s (40 ft/s). The ratio of the transverse flow area in the upper plenum (Sect. A-A in Fig. 3.7) to the pipe area at the output test section turbine flowmeter is 3.57. Therefore, velocities in the vicinity of the shielded HTC may have been >3 m/s (10 ft/s). Note that neither the velocity nor void fraction data obtained at the outlet spool are considered to be direct indications of the fluid conditions at the HTC sensor location because of the significant geometry differences between the HTC location and the outlet spool piece. These flow conditions correspond to high-void-fraction flow with the reactor coolant pump running. Under those conditions, the rod bundle power required to achieve DNB was >13 kW/m (4 kW/ft). More details and data from these film boiling experiments are given in Ref. 8.

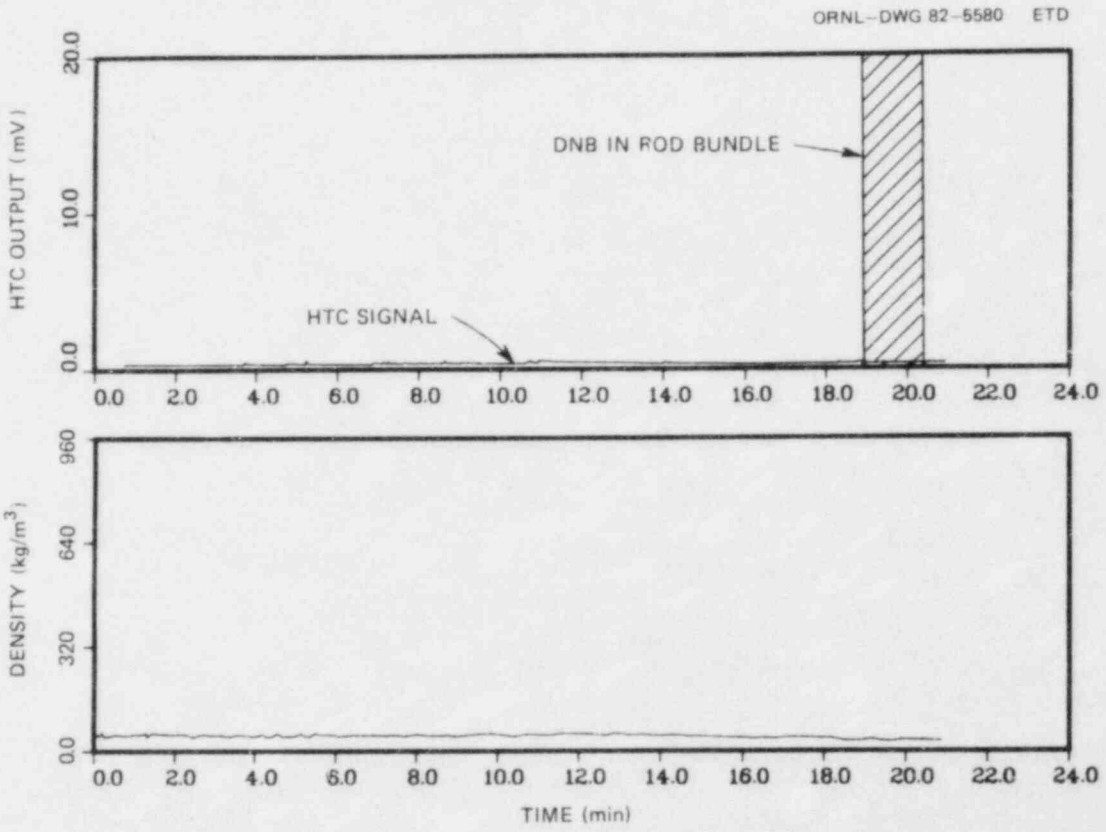

Fig. 4.23. Heated thermocouple output, measured density, and measured volumetric flow at test section outlet. Parts of the rod bundle were in film boiling at 19 min. Inlet flow was 4.15 L/s (66 gpm) and system pressure was 8.5 MPa (1230 psia).

Test parameters of the low-flow rod bundle heat transfer tests are given in Table 4.6. The THTF operating procedures for these tests were generally as follows: before power was applied to the FRS bundle, a base loop temperature was established by circulating water through the pump bypass loop. Then, the test section flow was reduced using a precision flow control valve, and power was applied to the rod bundle. Boiling occurred in the bundle, and the liquid level fell to the desired position, usually approximately one-fourth of the way down from the top of the heated length. In some cases, the system pressure was reduced in a prescribed manner during the boiloff (Table 4.6).

When the uncovery had reached its maximum extent, the system was allowed to reach a quasi-steady-state condition, and data were taken to investigate steam cooling effects. The reflood phase occurred when a flooding valve was opened and water at the base loop temperature entered the test section, eventually rewetting the bundle.

The most important questions to be answered by this series of HTC tests were as follows: (1) Could the HTC mechanically survive LOCA thermal-hydraulic environments for extensive periods? (2) Would the HTC output behavior correspond to that of the heated rod bundle? (3) What were

Table 4.6. Test points achieved in THTF Test 3.09.10

Test name[a]	Pressure (MPa)	Linear heat rate (kW/m)
UI	4.1	2.0
UJ	4.1	1.0
UK	4.1	0.3
UL	7.6	2.0
UM	7.6	1.0
UN	7.6	0.3
RO	4.1	2.0
RP	4.1	1.0
RQ	4.1	1.0
RR	7.6	2.0
RS	7.6	1.0
BT[b]	6.2 → 4.1	1.0
BU[c]	7.9 → 6.2	2.0
BV[c]	7.9 → 6.2	0.7
BW[b]	7.9 → 6.2	0.3
BX	8.6	0.7

[a] U denotes uncovery test; R denotes reflood test; B denotes boiloff test.

[b] Depressurization rate ≅14 kPa/s.

[c] Depressurization rate ≅21 kPa/s.

the flow conditions (e.g., pressure, mean velocity, and density) existing in the vicinity of the HTC at various times during the test?

Available information relating to these three test objectives follows.

1. The HTC survived THTF Test 3.09.10. After the test, both heater and TC circuits were intact and remained well insulated from each other and from ground.

2. and 3. Analysis of data obtained from the HTC and other facility instrumentation during Test 3.09.10 indicates that the HTC output consistently corresponded to the occurrence of high void fraction and poor cooling in the rod bundle (Figs. 4.24 and 4.25). Void fraction at the test section outlet (and, presumably, the test section upper plenum) was inferred from the outlet densitometer reading. Rod bundle temperatures were observed during the test using a cathode ray tube (CRT) display in the THTF control room. Test section outlet velocities for Test 3.09.10 were

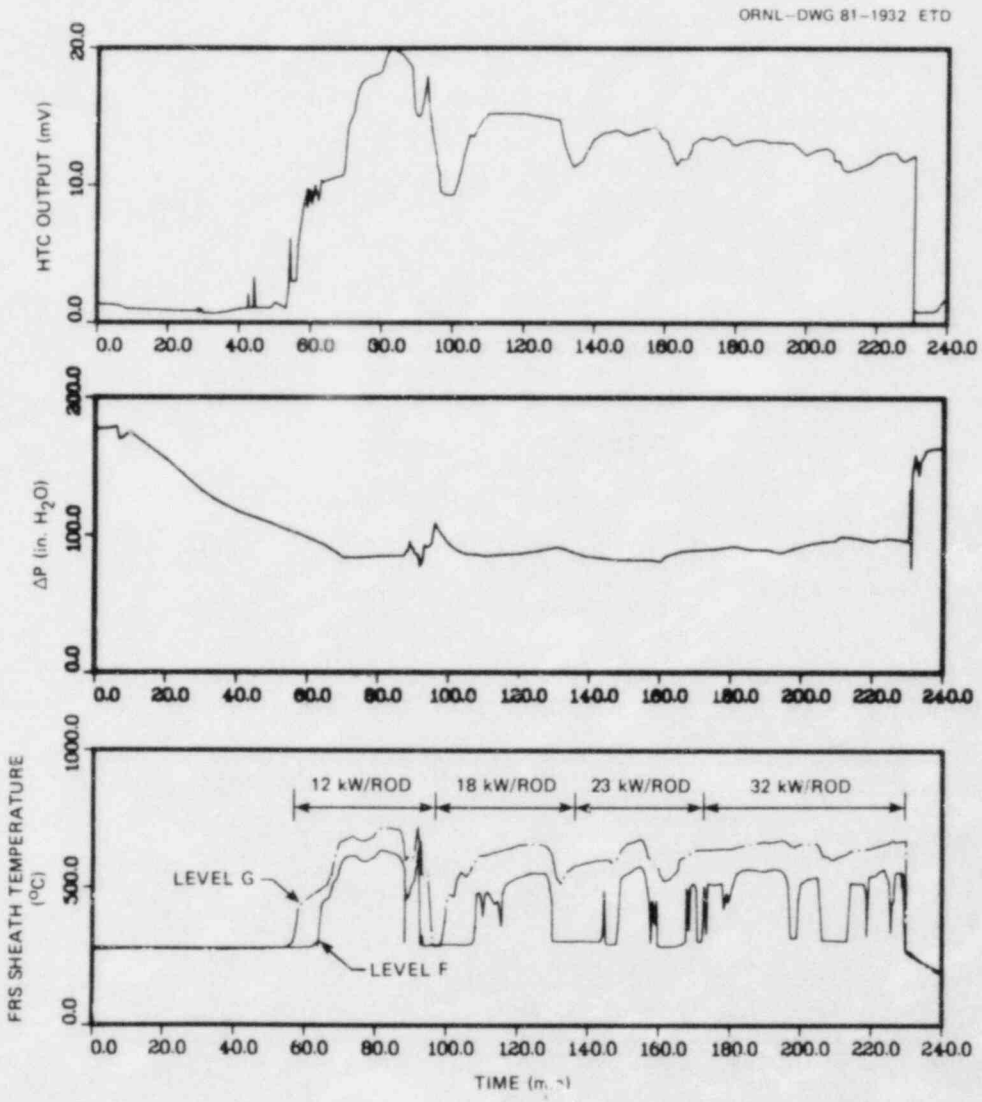

Fig. 4.24. (a) HTC output, (b) ΔP reading, and (c) FRS sheath TC readings at two bundle levels during THTF rod bundle boiloff and reflood test series.

significantly lower than those observed during Test 3.07.9. The maximum outlet spool velocity observed during Test 3.09.10 was ~0.7 m/s. (Outlet velocities greater than ~3 m/s during Test 3.07.9 resulted in continuous cooling of the HTC, independent of bundle cooling conditions.)

The THTF tests suggest that a reactor core at an intermediate power level (e.g., 15 kW/m) may indeed become inadequately cooled. This was evidenced by high rod surface temperatures during THTF Tests 3.07.9 even though high outlet flow rates were measured. However, these high flows were sufficient to cool the HTC, thus causing an incorrect indication. Apparently, the HTC (as tested) is capable of ICC detection, if the core power level is at decay heat values. This occurs because the high flow

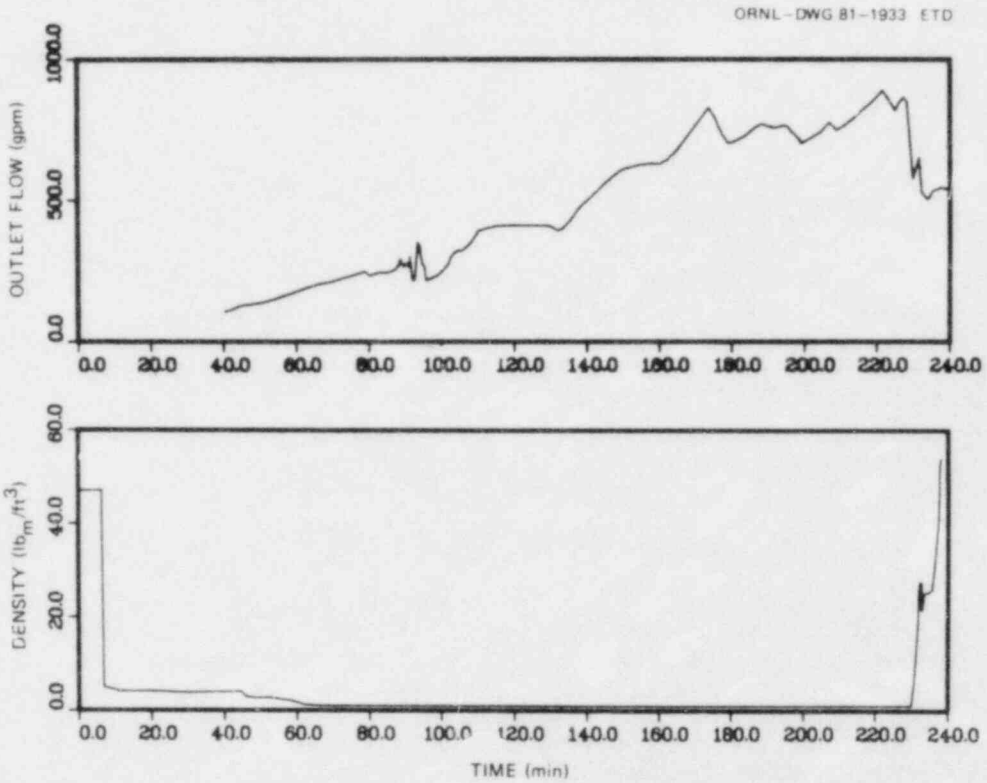

Fig. 4.25. (a) Measured volume rate of flow and (b) density obtained during THTF rod bundle boiloff and reflood test series.

rates that caused unreliable HTC reading in Test 3.07.9 are sufficient to cool the rod bundle at low-power levels (Test 3.09.10).

The THTF testing indicated that further instrument development was needed if thermal-type sensors, located in a high-velocity two-phase flow field, are required to detect the presence of high void conditions (and poor cooling).

4.4 Splash Shield Testing

Tests of thermal devices in systems with natural and forced convection showed that some means was needed to protect the sensors from cooling by water droplets. A vertically oriented probe immersed in stagnant or flowing steam is likely to accumulate liquid films. Water then may fall downward to quench the probe's heated region. Observation showed also that both horizontal and vertical probes could be easily cooled by two-phase flow of steam and liquid water even when very little of the liquid phase was present. Several droplet or splash shields were fabricated and tested. Most of the testing involved probes consisting of a single horizontal cylinder. The objective was to find a shield that would allow a thermal probe with moderate heat input (with surface heat fluxes corresponding to nuclear decay heat values) to dry out in a high vapor fraction

flow field. Such a sensor might provide early warning of the approach to inadequate cooling in a PWR vessel. It would also be less susceptible to spurious rewetting and ambiguous indication caused by deentrainment of water on vessel internal structures.

A half cylinder was added to the HRTD to cover the top of the sensor from falling condensate. The effect of adding this shield was shown in Fig. 4.15. A simple hood greatly improved the probe results; however, this test was in stagnant steam.

Both MPHJTC arrays were provided with splash shields (Figs. 2.4 and 2.5). The shield around the three-element array was a 12.7-mm-OD tube with 0.9-mm walls. The HTC OD was 6.4 mm. The annulus formed was 2.25 mm wide. The test results showed that the annular region was apparently sufficient to allow transfer of water inside the shield so that the interior level corresponded to the exterior level. However, the shield may have reduced heat transfer coefficients on the probe surface in the vicinity of the liquid level, making the probe less sensitive to heat transfer effects at the surface. The splash shield surrounding the four-element array had a 10.8-mm OD with 0.64-mm walls. The annulus gap around the 6.7-mm-OD probe was 1.42 mm. Holes 3.2 mm in diameter were drilled along the length to allow water to enter and drain. Test results indicated that water was transferred to and from this shield. Note that, for both arrays, the test conditions were static steam and water.

Another of the shields tested is shown in Fig. 4.26. Two slots were located opposite the heated region of the probe and in the same horizontal plane as the probe center line. Additional vents were made above and below the probe on the opposite end of the probe from the heated region.

Bench tests showed that water in the annulus between the probe and the shield was difficult to drain. Tests were run in the AIRS test stand with an HTC (ORNL II) incorporating the splash shield. The test conditions approximated those used when the same probe, without the splash shield, was tested previously. Probe response was again found to be insensitive to void fraction and flow velocity in two-phase flow. The output ΔTs for the tests with shield in place were approximately twice those

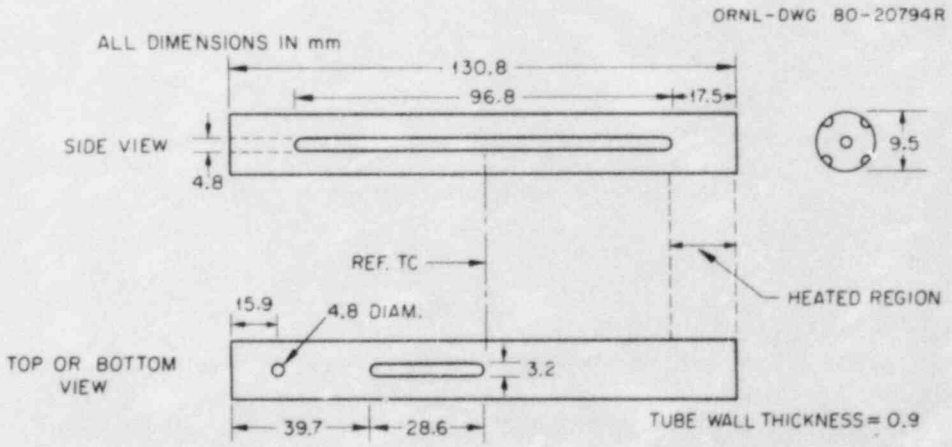

Fig. 4.26. Schematic of splash shield used with ORNL II probe.

observed without the shield; however, even with the same heater power, high-void-high-velocity flows still could not be clearly distinguished from a liquid flow.

To understand why a splash shield does or does not work, two special experiments were conducted. The first involved an HTC with a splash shield that consisted of a cylinder with two drain holes. This apparatus was tested in mist flow at various velocities. The second experiment involved a standpipe that is essentially a hollow tube with holes to allow communication with the surrounding media. The testing investigated the ability of the standpipe to measure the collapsed liquid level of a flowing two-phase mixture. If a standpipe functions well, it might be used as a shield for a thermal sensor.

The HTC was tested under mist-flow conditions in the 3-Mod A/W IDL and a bench-scale setup.

An HTC with a splash shield was placed into the upper plenum of the 3-Mod A/W IDL. The IDL represents a part of a vertical section from a PWR, including a short length of dummy fuel rods, upper end boxes, core support plate, and control rod guide tubes (Fig. 3.2). A low-energy gamma densitometer was located at approximately the same vertical height as the HTC. The loop was run to produce a mist flow in the upper plenum. The output of the shielded HTC was monitored in conjunction with the gamma densitometer. The results of four tests are presented in Table 4.7. At moderate air flows, the HTC showed significant cooling at very high void levels ($\alpha \simeq 0.979$). This points out the possibility that the HTC may indicate adequate cooling where it may not exist.

Table 4.7. Mist flow test results for the HTC in high-void-fraction air/water flow

Run No.	Densitometer void fraction (α)	HTC output (mV)
1	0.00	0.75
2	0.998	9.0
3	0.979	2.5
4	0.967	1.0

In response to these HTC test results [i.e., appreciable cooling at high-void-fraction flows ($\alpha \simeq 0.98$)], a second series of experiments was implemented. In these runs, a fine mist to a liquid stream was sprayed transverse to the shielded HTC well above the location of the thermal device. Care was taken to avoid spraying water droplets directly into the flow holes on the splash shield (Fig. 4.27). These relative positions of

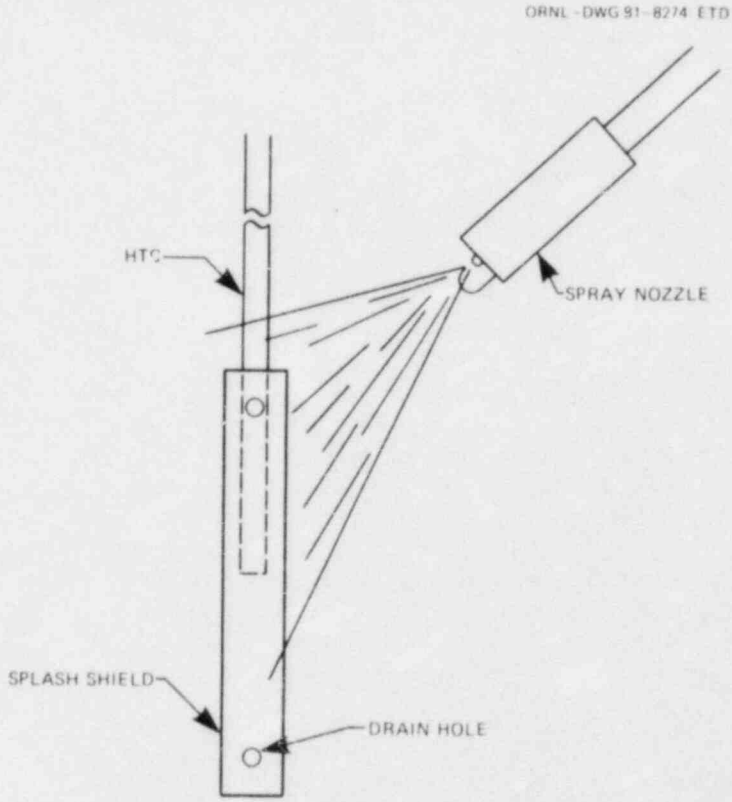

Fig. 4.27. Relative positions of HTC and spray nozzle.

the spray and probe caused any mist droplets that were collected on the HTC shield to flow down past the heater region and provide cooling. The water film or droplets that ran down the outside of the splash shield were collected in a graduated cylinder. The collected water was the flow available for cooling the HTC. To begin to understand the cooling effects of the mist, the collected water rate was compared with the ratio of

$$\Delta T_{spray}/\Delta T_{H_2O} ,$$

where ΔT_{spray} is the change in HTC output from the dry condition per first minute of water spray and ΔT_{H_2O} is the change in output from dry to water immersion. This comparison is illustrated in Fig. 4.28. Detectable cooling was observed when flow was only 0.03 mL/s, corresponding to a film Reynolds No. of 25.

For reasons not well understood, a fine mist can substantially cool a shielded heated device. The mist does not necessarily need to be traveling at high velocities. This is perplexing and adds to the uncertainty of whether heated thermal sensors are unambiguous or not.

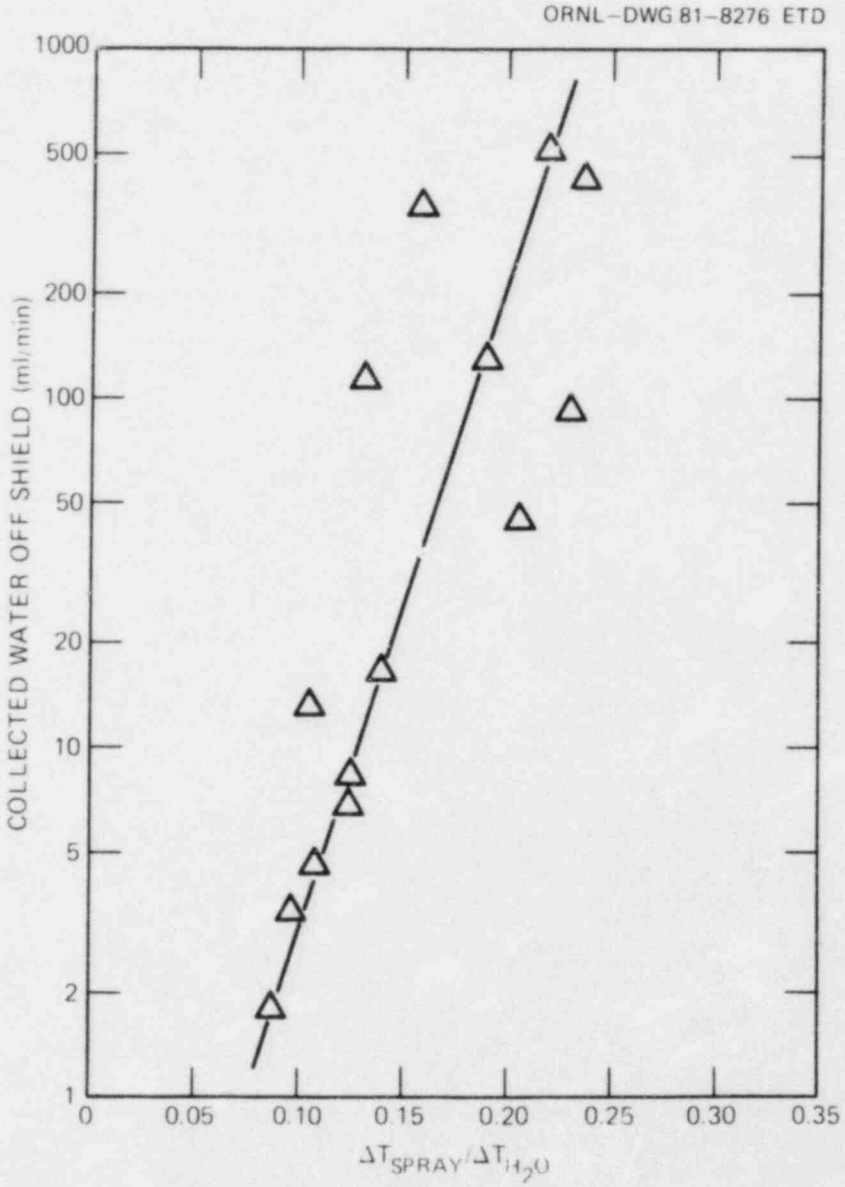

Fig. 4.28. Comparison of film rate on HTC shield with cooling rate of HTC in high void conditions.

A standpipe arrangement was run under two-phase flow conditions, and its collapsed liquid level was compared with the flowing voids as measured by a three-beam gamma attenuation densitometer.

In theory, a standpipe is a device that shields a thermal level detector, such as an HTC, from water droplets that splash directly on the thermal level detector and cause subsequent cooling. In practice, the standpipe consists of a tube closed at both ends with vent holes near the top and bottom. The pipe prevents droplets from spuriously cooling the thermal detector, and the vent holes afford communication between the flow

and the level detector. Several questions were considered:

1. Does the standpipe protect the thermal level detector?
2. Does it allow adequate time response?
3. Does it indicate a collapsed liquid level comparable with the actual flow?
4. Are there flow velocity effects?

To investigate the last two questions, a standpipe arrangement was designed, fabricated, and installed in the AWTF (Fig. 4.29). The collapsed liquid level in the standpipe was monitored by the sight glass mounted outside the test section. A three-beam gamma densitometer was located immediately downstream of the test section to measure the flowing void fraction. Collapsed liquid level data from the standpipe were compared with the center beam (B-beam) liquid fraction (Fig. 4.30). The

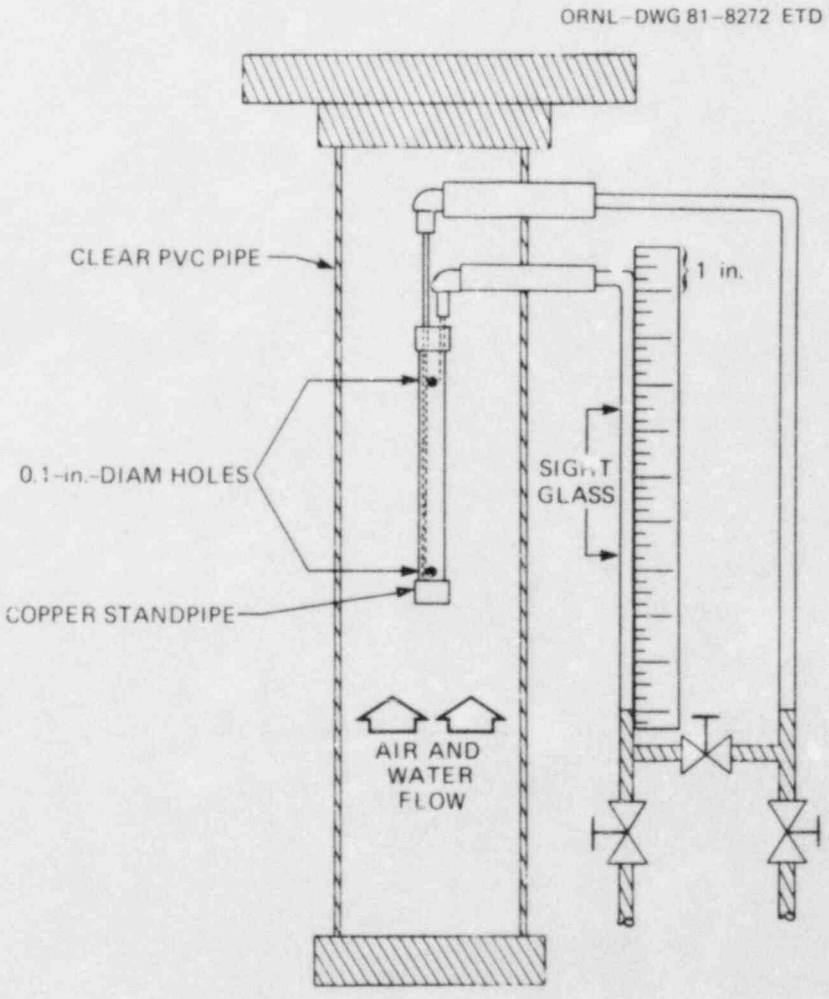

Fig. 4.29. Standpipe splash shield air/water test section.

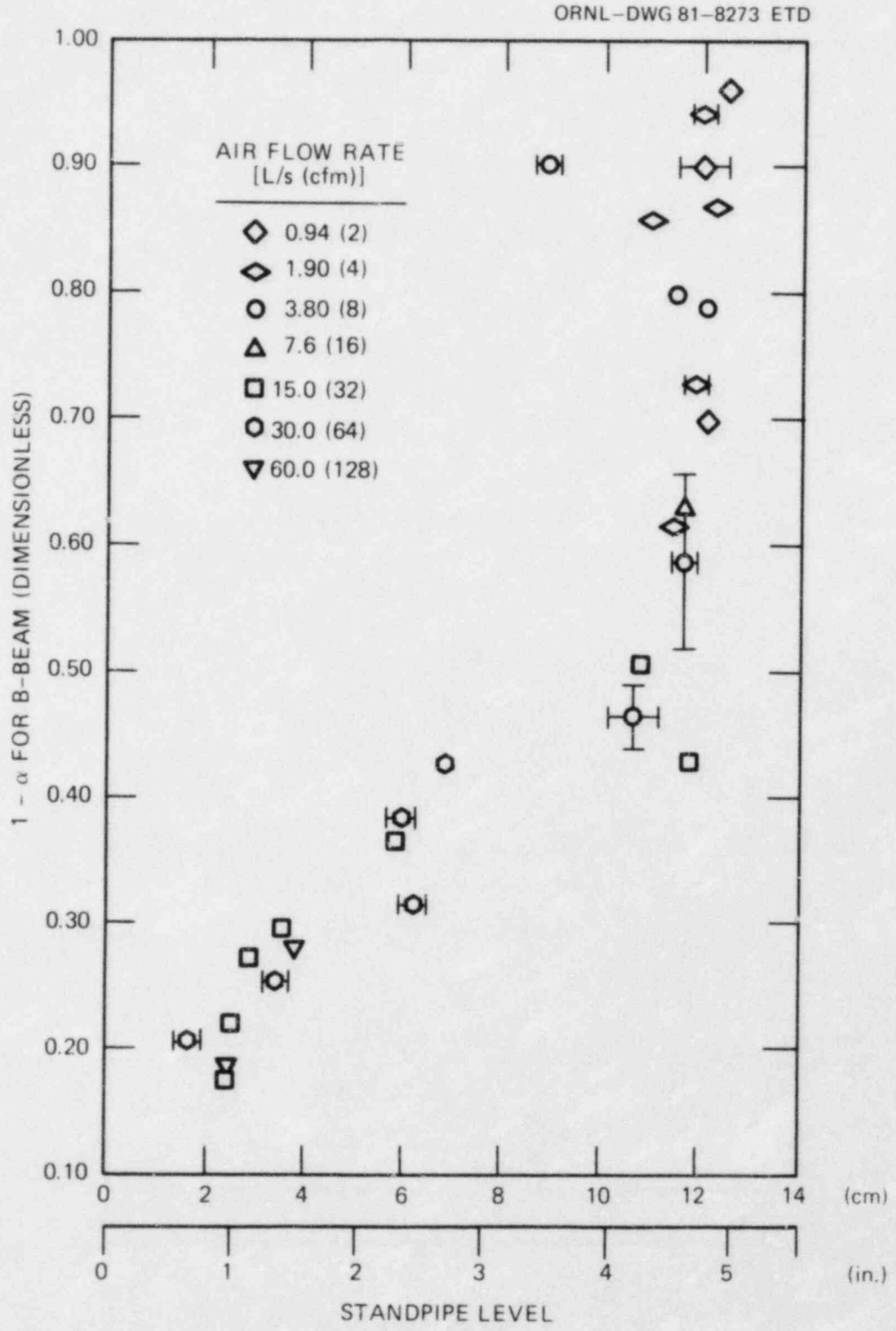

Fig. 4.30. Standpipe water level in vertical air/water flow vs liquid fraction from gamma densitometer.

level in the standpipe increases with rising liquid fraction as would be expected. The data scatter becomes much larger at the higher liquid fractions. The standpipe level data were transformed into liquid fraction by dividing the measured level by the distance between the pressure taps [13.3 cm (5.25 in.)]. This technique yields an average liquid fraction over the region between the taps, whereas the gamma densitometer yields a local point value. However, the distance between pressure taps is relatively short; thus, discrepancies caused by averaging are expected to be small. The comparison of standpipe liquid fraction with that of B-beam is shown in Fig. 4.31. Generally good agreement is noted in low liquid fraction range ($\beta < 0.40$ by the densitometer), but considerable scatter arises at high liquid fractions. This scatter may, in part, be attributed to the increasing portion of the pressure drop that is caused by friction. Rough estimates indicated that at high liquid fractions, 20% of the pressure drop was caused by flow. This added pressure increases the level in the

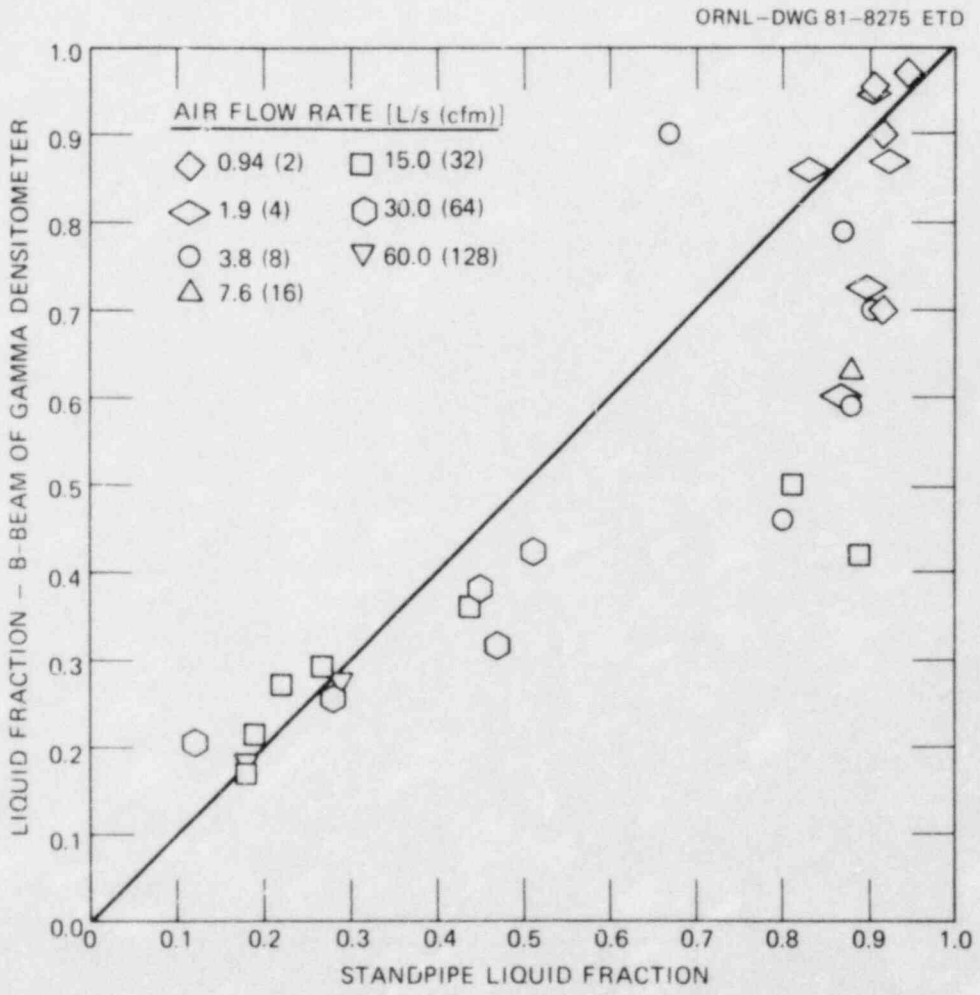

Fig. 4.31. Comparison of liquid fraction from standpipe and gamma densitometer.

standpipe and is then interpreted as more liquid present than is the case. The collapsed liquid level in this case would provide a nonconservative estimate of the void fraction. Thus, certain flow conditions (high-liquid fraction or high-velocity, high-void flows) may lead to the standpipe yielding an erroneous level and causing the thermal device to give incorrect indications.

4.5 Comparison of ΔP Technique with an HTC in THTF

During part of the THTF bundle boiloff-reflood test sequence, chart recordings were made using some additional instrument signals: (1) two FRS sheathed thermocouples in the upper bundle, (2) a test section ΔP instrument, (3) the HTC described previously, and (4) the turbine and densitometer at the test section outlet. The FRS temperature measurements were made at levels F and G, located 63.5 and 3.2 cm below the top of the bundle heated length, respectively. The two taps used in the ΔP measurements were located in the upper plenum, 57 cm above the top of the bundle heated length, and in the lower plenum, 34 cm below the bottom of the 3.66-m-long bundle. A Model 1151 DP Rosemount ΔP transducer was used.

Data from these instruments are plotted in Figs. 4.24 and 4.25. System pressure during the 4-h period ranged from ~6.2 to 8.3 MPa (900 to 1200 psia). Test section inlet flow rates were varied in steps from 0.32 to 1.2 L/s (5 to 19 gpm); the inlet fluid temperature was slightly subcooled. The FRS bundle power was cycled to produce partial bundle uncovery, then partial reflood and rewet on several occasions (Fig. 4.24). Higher bundle powers were used with the higher flow rates as indicated. The FRS sheath temperatures (approximately equal to FRS surface temperatures) varied from just above saturation (the flat portions of the temperature plots) to ~700°C (1300°F).

A densitometer installed on the horizontal outlet nozzle was used from time t = 0 to t = 35 min (Fig. 4.25). Stratified flow apparently occurred in that pipe, and the liquid level fell below the densitometer beam at ~7 min. Subsequently, the void fraction at the outlet was $\geq$50%. Beginning at t = 35 min and continuing for the remainder of the test, the signal from the downstream densitometer was used. This densitometer was mounted on a vertical pipe so that no problem with flow stratification existed. By t = 55 min, the test section outlet density indicated that saturated or superheated steam was present. The outlet volumetric flow rate increased during the test, reflecting the increase in test section mass flux. The maximum flow velocity indicated by the turbine during the test was ~3 m/s (10 ft/s) at 240 min.

The HTC response was very similar to that observed during previous tests. Output ΔT increased rapidly from ~1 to 10 mV at t = ~55 min. This preceded by a few minutes the occurrence of critical heat flux (CHF) at level G in the FRS bundle. Some sporadic signal spikes, probably caused by brief dryout and rewet of the HTC, occurred during the ~30-min period before the HTC dryout.

Output from the FRS TC at level G and the outlet densitometer suggests that the uppermost part of the bundle did not completely rewet during the test except for a few minutes at t = 100 min. Level F quenched

several times during the test. Although the HTC output remained high, variations in its output correspond in time to variations in the degree of FRS cooling. For instance, partial bundle rewets at t = 95, 130, and 160 min are easily seen in both the HTC output and the FRS TC temperature The rewets probably produced a burst of steam with entrained liquid effectively cooled the upper bundle and the HTC. At t = 230 min, the bundle power was tripped, the bundle reflooded, and the HTC output decreased to 1 mV.

Measurements of the ΔP across the rod bundle also provided information on liquid inventory. For a low-flow-rate condition such as this, the ΔP caused by hydraulic friction is relatively small. Also, the upper ΔP tap is located in the plenum so that velocities and dynamic pressure may be neglected. The measured ΔP (Fig. 4.24) during the boiloff-reflood tests qualitatively shows the depletion of bundle liquid inventory. For instance, the existence of voids detected by the outlet densitometer during the period ~0 to 50 min is indicated by continuous reduction in pressure drop. Interpretation of ΔP variations during the boiloff-reflood period is more difficult; variations in the ΔP signal appeared relatively small until total bundle reflood occurred at 230 min. During the 70- to 230-min period, the collapsed liquid level indicated by the ΔP system varied between 172 and 227 cm above the bottom of the heated length, or 75 to 130 cm below level F. The top of the froth level in the bundle was probably higher than this, as evidenced by the rewets at level F on several occasions.

Based on this test, some preliminary conclusions about the utility of HTCs and ΔP systems for detection of poor cooling may be reached: (1) Either method may be used to provide an indication of loss of liquid inventory if the transient is relatively slow and core power is at or below maximum decay heat levels. (2) In such a transient, the ΔP method may provide earlier warning (relative to the HTC) of the existence of voids (steam) in the primary system; that is, the ΔP responds at a lower void fraction than the HTC. (3) The HTC may give more reliable or more easily interpretable information than the ΔP regarding changes in the extent of core uncovery during an accident.

These results might be different for more rapid transients, for different HTC sensor designs or installation methods, or for different ΔP system configurations.

5. SUMMARY OF RESULTS

The use of heated thermal sensors for monitoring the coolant level in reactor vessels has been investigated. Several designs of thermal devices were examined, including HTCs and HRTDs. Several types of HTCs in both single-element and multiple-element arrays were fabricated at ORNL for these tests. Also, thermal sensors procured from various sources outside the laboratory (such as C-E, FCI, and Naval Reactors Program) were tested.

Several techniques for powering and controlling thermal devices were studied. All of the techniques were shown to be viable, with each having certain advantages and disadvantages. For example, using the differential output from the sensors to maintain a constant temperature can protect the heater when exposed to vapor for prolonged periods. However, this scheme requires a more complex control system and a higher price. Trade-offs must be made with any technique, and selection of one must be based on the particular requirements of the measurement.

All of the thermal devices tested at ORNL in natural convection proved to be reliable in that they were able to detect the presence or absence of adequate cooling. Also, with proper shielding from condensate, the data from the sensors were repeatable. Testing included pressures from 0.1 to 10.8 MPa and temperatures from 28 to 315°C. The devices that were investigated were: (1) single-element HTCs, (2) single-element HRTDs, and (3) multiple-position HTC arrays.

Testing of the HTCs revealed that the density of the probe internal insulation (usually MgO) was important. Results indicated that the more dense the insulation filler was made (i.e., more tightly compacted), the better. This compactness tended to increase the ratio of radial heat transfer to axial heat transfer. By swaging the probe, the filler material is compacted (fewer voids) and the radial heat transfer is increased. Because of the design and fabrication of ORNL HTCs, the swaging operation has little or no effect on the axial heat transfer rate. By establishing a higher ratio between the radial and axial heat transfer, there is relatively less heating of the reference TC junction by an adjacent heater, thus maintaining a reasonable resolution in detecting surface heat transfer (and ultimately liquid level).

The tests performed in forced convection indicated that only a small amount of liquid is required to cool unshielded thermal sensors operating at decay heat power rates. This cooling phenomenon occurred in heated rod bundle experiments in the THTF. Although this occurrence is not ambiguous in that the sensor indicates adequate cooling when, in fact, poor cooling conditions exist, the fact that the unshielded thermal device has low ΔT outputs in high void flows would preclude its use in detecting approach to ICC under these conditions. To detect the approach to ICC, some means to reliably isolate the sensors (splash shield or standpipe) must be developed.

Test results from THTF film boiling and low-flow rod bundle heat transfer experiments with an HTC were as follows:

1. Thermal sensor remained operable after more than 40 h at LOCA conditions.

2. The sensor indicated poor cooling prior to and during rod bundle dryout at 4, 6, 8, and 12 MPa (600, 900, 1200, and 1800 psi) with outlet velocities to ~3 m/s (10 ft/s).
3. The HTC failed to show inadequate cooling while parts of the rod bundle were drying out. This occurred at higher velocities (>3 m/s) and bundle powers.

To protect a thermal probe from condensate or the liquid-phase present in the flow stream, some sort of shielding is necessary. The testing at ORNL has shown that the design of a suitable shield (splash shield or standpipe) is very much an art. Several types of shields were investigated; most proved to be inadequate. The most successful shield tested consisted of a hollow cylinder with small vent or drain holes. This design, however, was not without problems. Mist flowing at relatively low velocities across a shielded HTC produced substantial cooling. Obviously, the basic fundamentals as to how and why shields function or do not function are not well understood at this time.

Preliminary comparisons between HTCs and ΔP measurements for coolant level detection during THTF tests suggest that for slow transients

1. both techniques yield advance warning and reliably detect low liquid level;
2. ΔP provides earlier indication of voiding (approach to ICC); and
3. after initial dryout in a bundle, HTCs may be more sensitive to changes in core froth level.

In summary, thermal devices appear to fulfill several of the requirements for PWR liquid level instrumentation. The sensors can (1) be made reliable, having long life and surviving LOCA conditions; (2) respond to changes in coolant conditions in a matter of seconds; and (3) be fabricated in arrays to cover the necessary in-vessel elevation range. However, as testing has shown, conditions exist (high void fraction and high velocity flows in particular) where incorrect indications are given by thermal probes. In most cases, a useful response is produced by the sensors, but as tested, thermal sensors are not absolutely unambiguous in high velocity flows.

6. RECOMMENDATIONS

To increase the usefulness of thermal probes and reduce the chance of ambiguous responses, development of means to isolate the sensor from the cooling effect of the liquid phase is imperative. Increased knowledge of the flow hydrodynamics around shielding is essential in designing an adequate device.

Improved understanding of the heat transfer from the thermal device to its surrounding media would be most helpful. A dynamic model of a thermal probe to predict the response of the sensor under not only stagnant steam and water conditions, but also under flowing steam and water mixtures, would be an important design tool.

If testing and modeling were done in the above two areas, important advances toward making thermal sensors reliable and unambiguous could result.

REFERENCES

1. *TMI-2 Lessons Learned Task Force Status Report and Short-Term Recommendation*, NUREG-0578, pp. A.11-12 (July 1979).

2. *NRC Action Plan Developed as a Result of the TMI-2 Accident*, NUREG-0660, Sects. 1.D.5 and 2.F.2 (May 1980).

3. *1967 Steam Charts*, p.61, Electric Research Association, St. Martin Press, NY, 1968.

4. *Project Description ORNL PWR Blowdown Heat Transfer Separate Effects Program - Thermal-Hydraulic Test Facility (THTF)*, ORNL/NUREG/TM-2 (NRC-1, -2) (February 1976).

5. F. J. Homan and P. R. Kasten, *Gas-Cooled Reactor Program Annual Report for the Period Ending December 31, 1977*, ORNL-5412, pp. 115-121.

6. J. R. S. Thom et al., "Boiling in Subcooled Water During Flow Up Heated Tubes or Annuli," pp. 226-246 in *Proceedings of the Institute of Mechanical Engineers, London*, 180 (Part 3C), Institute of Mechanical Engineers (1966).

7. J. D. White et al., *Quarterly Progress Report on Blowdown Heat Transfer Separate-Effects Program for July-September 1980*, NUREG/CR-1837 (ORNL/NUREG/TM-425).

8. K. G. Turnage et al., *Preliminary Report on Heated Thermocouple Response During Thermal-Hydraulic Test Facility Test 3.07.9 Quasi-Steady-State Film Boiling*, ORNL, unpublished internal document (December 1980).

NUREG/CR-2673
ORNL/TM-8306
Dist. Category R2

Internal Distribution

1. J. L. Anderson
2-6. R. L. Anderson
7. W. G. Craddick
8. D. S. Griffith
9-13. J. E. Hardy
14. H. W. Hoffman
15. T. S. Kress
16. A. L. Lotts
17. G. N. Miller
18. F. R. Mynatt
19. H. E. Trammell
20. ORNL Patent Office
21. Central Research Library
22. Document Reference Section
23-24. Laboratory Records Department
25. Laboratory Records (RC)

External Distribution

26. C. W. Connell, Jr., Babcock & Wilcox, Nuclear Power Generation Division, Lynchburg, VA 24505
27. R. E. Bryan, Combustion Engineering, 1000 Prospect Hill Road, Windsor, CT 06095
28. W. G. Lyman, Westinghouse Electric Company, Monroeville Nuclear Center, P.O. Box 355, Pittsburgh, PA 15230
29-36. Director, Division of Accident Evaluation, Nuclear Regulatory Commission, Washington D.C. 20555
37. Director, Reactor Division DOE, ORO, Oak Ridge, TN 37830
38. Office of Assistant Manager for Energy Research and Development, DOE, ORO, Oak Ridge, TN 37830
39-43. Director, Reactor Safety Research Coordination Office, DOE, Washington, D.C. 20555
44. H. D. Wills, General Electric, 175 Curtner St., MC 214, San Jose, CA 94303
45. P. G. Bailey, Electric Power Research Institute, P.O. Box 10412, Palo Alto, CA 94303
46-47. Technical Information Center, DOE, Oak Ridge, TN 37830
48-392. Given distribution as shown in category R2 (10-NTIS)
393-430. Special NRC External Distribution

☆U.S. GOVERNMENT PRINTING OFFICE: 1982-546-067/132